

## Alkaline Earth Metals | Hot Paper |

## Highly Fluorinated Tris(indazolyl)borate Silylamido Complexes of the Heavier Alkaline Earth Metals: Synthesis, Characterization, and Efficient Catalytic Intramolecular Hydroamination

Nuria Romero,<sup>[a, b]</sup> Sorin-Claudiu Roșca,<sup>[c]</sup> Yann Sarazin,<sup>[c]</sup> Jean-François Carpentier,<sup>[c]</sup> Laure Vendier,<sup>[a, b]</sup> Sonia Mallet-Ladeira,<sup>[d]</sup> Chiara Dinoi,<sup>\*[a, b]</sup> and Michel Etienne<sup>\*[a, b]</sup>

**Abstract:** Heteroleptic silylamido complexes of the heavier alkaline earth elements calcium and strontium containing the highly fluorinated 3-phenyl hydrotris(indazolyl)borate  $\{F_{12}\text{-Tp}^{4Bo,3Ph}\}^-$  ligand have been synthesized by using salt metathesis reactions. The homoleptic precursors  $[Ae\{N(\text{SiMe}_3)_2\}_2]$  ( $Ae = \text{Ca}, \text{Sr}$ ) were treated with  $[\text{Ti}(F_{12}\text{-Tp}^{4Bo,3Ph})]$  in pentane to form the corresponding heteroleptic complexes  $[(F_{12}\text{-Tp}^{4Bo,3Ph})Ae\{N(\text{SiMe}_3)_2\}_2]$  ( $Ae = \text{Ca}$  (**1**);  $\text{Sr}$  (**3**)). Compounds **1** and **3** are inert towards intermolecular redistribution. The molecular structures of **1** and **3** have been determined by using X-ray diffraction. Compound **3** exhibits a  $\text{Sr}\cdots\text{MeSi}$  agostic distortion. The synthesis of the homoleptic THF-free

compound  $[\text{Ca}\{N(\text{SiMe}_2\text{H})_2\}_2]$  (**4**) by transamination reaction between  $[\text{Ca}\{N(\text{SiMe}_3)_2\}_2]$  and  $\text{HN}(\text{SiMe}_2\text{H})_2$  is also reported. This precursor constitutes a convenient starting material for the subsequent preparation of the THF-free complex  $[(F_{12}\text{-Tp}^{4Bo,3Ph})\text{Ca}\{N(\text{SiMe}_2\text{H})_2\}_2]$  (**5**). Compound **5** is stabilized in the solid state by a  $\text{Ca}\cdots\beta\text{-Si-H}$  agostic interaction. Complexes **1** and **3** have been used as precatalysts for the intramolecular hydroamination of 2,2-dimethylpent-4-en-1-amine. Compound **1** is highly active, converting completely 200 equivalents of aminoalkene in 16 min with 0.50 mol% catalyst loading at 25 °C.

## Introduction

The synthesis of nitrogen-containing molecules through metal-catalyzed hydroamination of C–C multiple bonds offers a perfectly atom-economic route to the production of fine chemicals.<sup>[1]</sup> Whereas the catalytic activity of transition metal and rare earth complexes for the addition of a N–H bond across C–C multiple bonds has been largely described in the literature,<sup>[2–6]</sup> the use of alkaline earth (Ae) metal complexes as hydroamination catalysts is only now starting to emerge.<sup>[7,8]</sup> Ae metals are abundant, oxophilic, and redox-inactive in their cationic form. They are characterized by a wide range of ionic

radii and cation charge densities ( $\text{Mg}^{2+} = 0.72 \text{ \AA}$ ;  $\text{Ca}^{2+} = 1.00 \text{ \AA}$ ;  $\text{Sr}^{2+} = 1.18 \text{ \AA}$ ,  $\text{Ba}^{2+} = 1.35 \text{ \AA}$  for six-coordinate ions).<sup>[9]</sup> Their chemistry is therefore largely governed by electrostatic and steric factors, featuring highly ionic and essentially non-directional bonding. One consequence is the deleterious Schlenk equilibrium that redistributes ligands in a heteroleptic complex  $[(L_nX)AeX']$  yielding a mixture of the two homoleptic species  $[(L_nX)_2Ae]$  and  $[AeX'_2]$  (Scheme 1). This equilibrium is often problematic for catalysis, and its control by the appropriate choice of ligands remains a challenge in this chemistry.



Scheme 1. Schlenk-type equilibrium with heteroleptic Ae complexes.

Intermolecular hydroamination reactions are extremely challenging and only a limited number of reports involving Ae catalysts are available in the literature.<sup>[10–13]</sup> By contrast, the entropically favored intramolecular version of this process has been investigated in more detail.<sup>[13–22]</sup> Both homo and heteroleptic alkaline earth complexes are competent cyclohydroamination precatalysts and, in general, the activity trend observed for such reactions is  $\text{Ca} > \text{Sr} > \text{Ba}$ ; on the other hand, no definitive trend in their reactivity with respect to the nature of the ancillary ligands emerges so far. With the readily available homoleptic compounds  $[M\{N(\text{SiMe}_3)_2\}_2(\text{thf})_x]$  ( $M = \text{Ca}, \text{Sr}, \text{Ba}$ ;  $x = 0$  or 2), the THF-free complexes displayed lower catalytic activity

[a] N. Romero, Dr. L. Vendier, Dr. C. Dinoi, Prof. M. Etienne  
CNRS, LCC (Laboratoire de Chimie de Coordination)  
BP 44099, 205 route de Narbonne, 31077 Toulouse Cedex 4 (France)  
E-mail: michel.etienne@lcc-toulouse.fr  
chiara.dinoi@lcc-toulouse.fr

[b] N. Romero, Dr. L. Vendier, Dr. C. Dinoi, Prof. M. Etienne  
Université de Toulouse, UPS, INPT, LCC  
31077 Toulouse Cedex 4 (France)

[c] S.-C. Roșca, Dr. Y. Sarazin, Prof. J.-F. Carpentier  
Institut des Sciences Chimiques de Rennes  
UMR 6226 CNRS-Université de Rennes 1  
Campus de Beaulieu, 35042 Rennes Cedex (France)

[d] S. Mallet-Ladeira  
Institut de Chimie de Toulouse (FR 2599), Université Paul Sabatier  
118 route de Narbonne, 31062 Toulouse Cedex 9 (France)

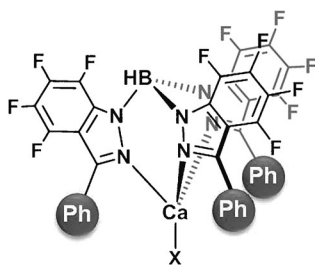
Supporting information for this article is available on the WWW under <http://dx.doi.org/10.1002/chem.201405454>.

than their THF-containing analogues, except in the case of substrates with secondary amine functionalities; moreover, the strontium systems were less active than their calcium counterparts.<sup>[15]</sup>

For the heteroleptic Ae species, very bulky ancillary donating ligands, capable of stabilizing the oxophilic metal center while providing the steric protection needed to prevent the Schlenk equilibrium, were employed. The catalytic activities of the heteroleptic silylamido  $\beta$ -diketiminato derivatives [(BDI)M{N(SiMe<sub>3</sub>)<sub>2</sub>}(thf)<sub>x</sub>] ((BDI)H = H<sub>2</sub>C[C(Me)N-2,6-(iPr)<sub>2</sub>C<sub>6</sub>H<sub>3</sub>]<sub>2</sub>; M = Ca, x = 0 or 1; M = Sr, x = 1) provided useful insight into the mechanism of the reaction.<sup>[14,15]</sup> The Ca precatalyst exhibited better catalytic performances than its Sr analogue. In contrast, the hydrobis and tris(imidazol-2-ylidene-1-yl)borates, containing C-based donors instead of N-based donors in the tripodal ligand, resulted in the Sr silylamido complexes performing better than their Ca counterparts. With the N-bound aminotroponimate or 2,5-bis-[N-(aryl)iminomethyl]-pyrrolyl Ca and Sr silylamido complexes, the activity of the catalysts decreased with increasing atomic number of the metal.<sup>[16–18]</sup> Asymmetric versions of these reactions have also been reported.<sup>[19–21]</sup>

Some of us have recently described new Ca, Sr, and Ba heteroleptic [(LO)Ae{N(SiMe<sub>2</sub>R)<sub>2</sub>}(thf)<sub>x</sub>] (R = H, Me) complexes bearing different types of N- and O-based amino-phenolate ligands (LO<sup>-</sup>). The rates for the cyclohydroamination reactions decreased with increasing atomic number of the metal.<sup>[22]</sup> For a given ligand framework and metal center, complexes that contain {N(SiMe<sub>3</sub>)<sub>2</sub>}<sup>-</sup> were much better precatalysts than those containing {N(SiMe<sub>2</sub>H)<sub>2</sub>}<sup>-</sup>.<sup>[22]</sup> Heteroleptic silylamido complexes [(N<sup>^</sup>N)Ae{N(SiMe<sub>3</sub>)<sub>2</sub>}(thf)<sub>x</sub>] (Ae = Ca, x = 1; Sr, Ba, x = 2) containing the bulky imino-anilide ligand {N<sup>^</sup>N}<sup>-</sup> also catalyzed the cyclohydroamination reaction efficiently, with rates increasing in the order Ba < Sr < Ca.<sup>[13]</sup>

We became interested in stabilizing electron-deficient heteroleptic alkaline earth complexes [(L<sub>n</sub>X)AeX'] while maintaining their reactivity. Our strategy is based on the use of highly fluorinated hydrotris(indazolyl)borate ligands ({F<sub>n</sub>-Tp<sup>4Bo,3Ph</sup>}<sup>-</sup>)<sup>[25–29]</sup> that combine two fundamental properties: 1) The steric hindrance, which would avoid Schlenk-type redistributions and 2) the electron-withdrawing ability, which would enhance the polarity, hence the reactivity of the Ae–X bond.<sup>[30]</sup> Two differently substituted ligands, {F<sub>n</sub>-Tp<sup>4Bo,3R</sup>}<sup>-</sup> (R = CF<sub>3</sub>, n = 21, and R = Ph, n = 12), have been tested on Ca, the phenyl-based ligand providing the best compromise in terms of steric protection and electron-withdrawing properties (Scheme 2).<sup>[31]</sup>



**Scheme 2.** The 3-Ph substituted hydrotris(indazolyl)borate ligand (X = reactive ligand).

Earlier reports have shown that sterically encumbered, differently substituted tris(pyrazolyl)borates (Tp') coordinate Ca<sup>2+</sup> with the formation of heteroleptic Tp'CaX complexes.<sup>[32]</sup> A four-coordinate amido complex [Tp<sup>4Bu</sup>Ca{N(SiMe<sub>3</sub>)<sub>2</sub>}] was obtained with Tp<sup>4Bu</sup>, whereas a five-coordinate THF adduct [Tp<sup>4Pr</sup>Ca{N(SiMe<sub>3</sub>)<sub>2</sub>}(thf)] was obtained with Tp<sup>4Pr</sup>.<sup>[33]</sup> These amido complexes were shown to catalyze the ring-opening polymerization of lactide,<sup>[33]</sup> but to our knowledge they have not been tested for hydroamination reactions.

We report here the synthesis of heteroleptic calcium and strontium silylamido complexes [(F<sub>12</sub>-Tp<sup>4Bo,3Ph</sup>)Ae{N(SiMe<sub>3</sub>)<sub>2</sub>}] (Ae = Ca; Sr), which are inert to intermolecular redistribution in solution. The synthesis of the homoleptic THF-free compound [Ca{N(SiMe<sub>2</sub>H)<sub>2</sub>}]<sub>2</sub> by a transamination reaction between [Ca{N(SiMe<sub>3</sub>)<sub>2</sub>}]<sub>2</sub> and HN(SiMe<sub>2</sub>H)<sub>2</sub> is also reported. This precursor has then been used for the preparation of [(F<sub>12</sub>-Tp<sup>4Bo,3Ph</sup>)Ca{N(SiMe<sub>2</sub>H)<sub>2</sub>}], which exhibits a Ca...β-Si–H agostic distortion. The catalytic activity of these amido complexes for the intramolecular hydroamination of 2,2-dimethylpent-4-en-1-amine is described. [(F<sub>12</sub>-Tp<sup>4Bo,3Ph</sup>)Ca{N(SiMe<sub>3</sub>)<sub>2</sub>}] is highly active, converting completely 200 equivalents of aminoalkene in 16 min at 25 °C.

## Results and Discussion

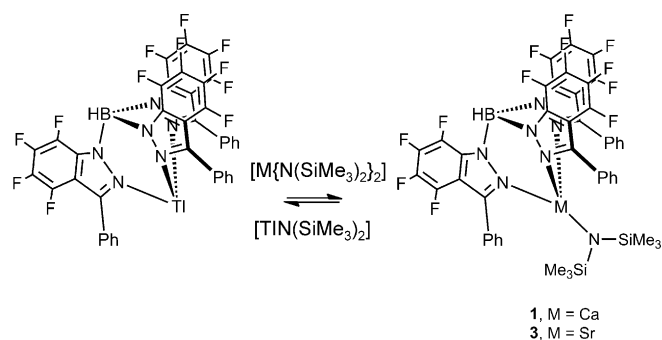
### Synthesis and characterization of

#### [(F<sub>12</sub>-Tp<sup>4Bo,3Ph</sup>)Ae{N(SiMe<sub>3</sub>)<sub>2</sub>}] (Ae = Ca, Sr)

Treatment of [Ti(F<sub>12</sub>-Tp<sup>4Bo,3Ph</sup>)] with an excess of [Ca{N(SiMe<sub>3</sub>)<sub>2</sub>}]<sub>2</sub> in pentane provided the heteroleptic [(F<sub>12</sub>-Tp<sup>4Bo,3Ph</sup>)Ca{N(SiMe<sub>3</sub>)<sub>2</sub>}] (**1**) in 67% yield. Compound **1** was characterized by standard analytical/spectroscopic techniques, and the solid-state structure was analyzed by single-crystal X-ray diffraction (see below). The <sup>19</sup>F NMR spectrum in [D<sub>6</sub>]benzene shows four signals (δ = –144.30, –151.59, –153.83, and –163.15 ppm) corresponding to the four benzo fluorine atoms of {F<sub>12</sub>-Tp<sup>4Bo,3Ph</sup>}<sup>-</sup>. The <sup>1</sup>H NMR spectrum displays one singlet for the Me groups of the {N(SiMe<sub>3</sub>)<sub>2</sub>}<sup>-</sup> amido ligand (δ = –0.34 ppm) and three multiplets (δ = 7.54, 7.32, and 7.23 ppm) for the aromatic protons of {F<sub>12</sub>-Tp<sup>4Bo,3Ph</sup>}<sup>-</sup>. From the equivalence of the three indazolyl groups of {F<sub>12</sub>-Tp<sup>4Bo,3Ph</sup>}<sup>-</sup> in solution, a time-averaged C<sub>3v</sub> symmetry can be inferred for **1**. The synthesis and purification of **1** proved to be challenging due to the involvement of an equilibrium process as summarized in Scheme 3 and Figure 1.

The homoleptic compound [Ca{N(SiMe<sub>3</sub>)<sub>2</sub>}]<sub>2</sub> was treated with [Ti(F<sub>12</sub>-Tp<sup>4Bo,3Ph</sup>)] in [D<sub>6</sub>]benzene affording **1** quantitatively over a period of 30 h (Figure 1 a–c). After evaporation of the solvent and re-dissolution in [D<sub>6</sub>]benzene, however, we observed the re-appearance of the characteristic signals of [Ti(F<sub>12</sub>-Tp<sup>4Bo,3Ph</sup>)] together with those of **1** (Figure 1 d), evidencing that the reverse reaction had occurred according to the equilibrium process in Scheme 3. [Ti(F<sub>12</sub>-Tp<sup>4Bo,3Ph</sup>)] is less soluble than **1** in [D<sub>6</sub>]benzene and its precipitation displaced the equilibrium towards the formation of the reactants.

The isolation of complex **1** was therefore achieved by carrying out the reaction in pentane. Due to their poor solubility,



Scheme 3. Equilibrium process involved in the synthesis of **1** and **3**.

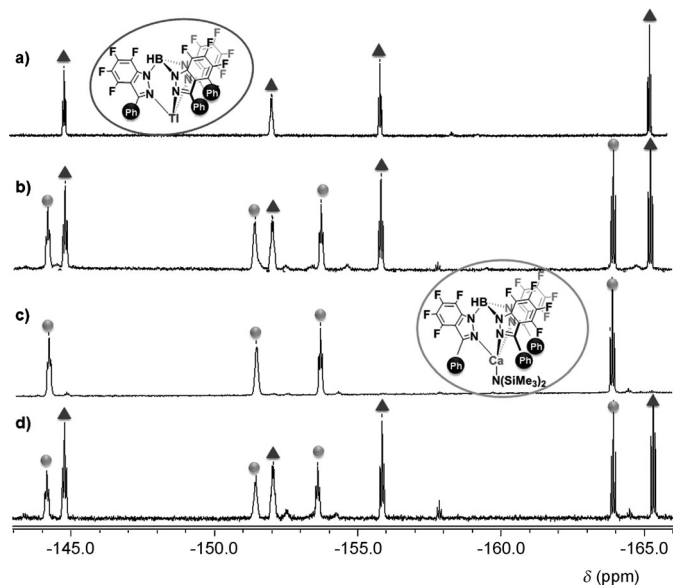


Figure 1.  $^{19}\text{F}$  NMR spectroscopic monitoring of the reaction of  $[\text{Ca}\{\text{N}(\text{SiMe}_3)_2\}_2]$  with  $[\text{Ti}(\text{F}_{12}\text{-Tp}^{4\text{Bo},3\text{Ph}})]$  in  $[\text{D}_6]$ benzene; a) Pure  $[\text{Ti}(\text{F}_{12}\text{-Tp}^{4\text{Bo},3\text{Ph}})]$ ; b) 1:1 Reaction mixture over a period of 3 h ( $\blacktriangle = [\text{Ti}(\text{F}_{12}\text{-Tp}^{4\text{Bo},3\text{Ph}})]$ ;  $\bullet = [\text{F}_{12}\text{-Tp}^{4\text{Bo},3\text{Ph}}]\text{Ca}\{\text{N}(\text{SiMe}_3)_2\}$ ); c) Reaction mixture over a period of 30 h; d) 1:1 Reaction mixture after evaporation and re-dissolution in  $[\text{D}_6]$ benzene.

$[\text{Ti}(\text{F}_{12}\text{-Tp}^{4\text{Bo},3\text{Ph}})]$  and complex **1** precipitated leaving  $[\text{Ca}\{\text{N}(\text{SiMe}_3)_2\}_2]$  and  $[\text{Ti}\{\text{N}(\text{SiMe}_3)_2\}]$  in solution. Following a simple filtration of the reaction mixture, complex **1** was then separated from  $[\text{Ti}(\text{F}_{12}\text{-Tp}^{4\text{Bo},3\text{Ph}})]$  by extraction with a toluene/pentane (1:3) mixture. The whole process was facilitated by using an excess of  $[\text{Ca}\{\text{N}(\text{SiMe}_3)_2\}_2]$  that further displaced the equilibrium towards the products. Compound **1** was finally isolated in 67% yield. Complex **1** is very air and moisture sensitive; small traces of air or water lead to immediate decomposition, with the formation of an unidentified white precipitate and  $\text{HN}(\text{SiMe}_3)_2$ . As a result of the presence of the bulky  $\{\text{F}_{12}\text{-Tp}^{4\text{Bo},3\text{Ph}}\}^-$  ligand, compound **1** was found to be inert towards the Schlenk equilibrium. Indeed, heating a  $[\text{D}_6]$ benzene solution of **1** at  $60^\circ\text{C}$  over a period of 2 h did not result in any apparent decomposition nor in ligand redistribution. Addition of THF to a  $[\text{D}_6]$ benzene solution of **1** suggested the formation of a mixture of THF amido species  $[(\text{F}_{12}\text{-Tp}^{4\text{Bo},3\text{Ph}})\text{Ca}\{\text{N}(\text{SiMe}_3)_2\}(\text{thf})_x]$ . Concentration under vacuum yielded, on the basis of  $^1\text{H}$  and  $^{19}\text{F}$  NMR spectroscopies, what

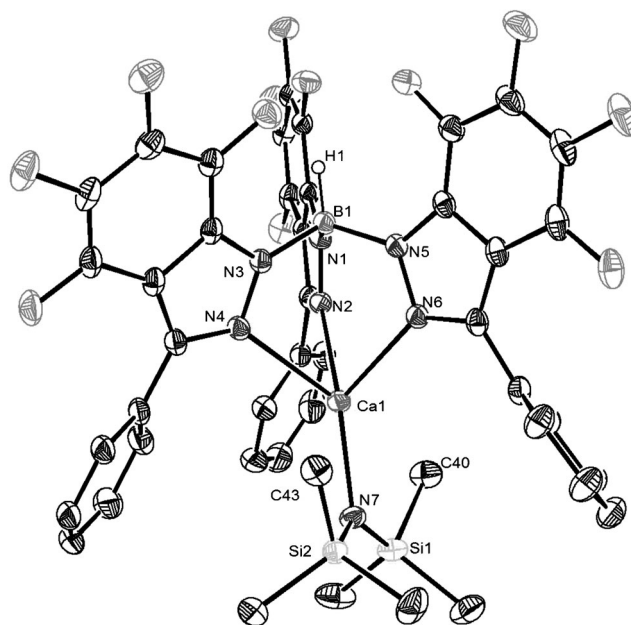


Figure 2. ORTEP drawing of  $[(\text{F}_{12}\text{-Tp}^{4\text{Bo},3\text{Ph}})\text{Ca}\{\text{N}(\text{SiMe}_3)_2\}]$  **1**. Selected bond lengths [Å] and bond angles [ $^\circ$ ]: Ca1–N7 2.2342(15), Ca1–N2 2.5084(14), Ca1–N4 2.4989(16), Ca1–N6 2.4566(15); N7–Ca1–N2 146.79(6), N7–Ca1–N4 126.94(5), N7–Ca1–N6 121.82(5), N2–Ca1–N4 71.79(5), N2–Ca1–N6 83.13(5), N4–Ca1–N6 85.49(5).

we suggest is  $[(\text{F}_{12}\text{-Tp}^{4\text{Bo},3\text{Ph}})\text{Ca}\{\text{N}(\text{SiMe}_3)_2\}(\text{thf})]$  (see below) as the major compound together with free indazole.

An ORTEP drawing of the solid state molecular structure of **1** is given in Figure 2 along with selected bond lengths and angles. Compound **1** has a monomeric structure where the Ca atom is four-coordinate in a distorted tetrahedral geometry. The B1, Ca1, and N7 (amido) atoms are almost collinear ( $165^\circ$ ). The distortion of the tetrahedron is such that Ca1–N<sub>indz</sub> bond lengths are longer for N2 and N4 (2.5084(14) and 2.4989(16) Å) than for N6 (2.4566(15) Å) and the angle N2–Ca1–N4 ( $71.79(5)^\circ$ ) is smaller than those involving N6 ( $83.13(5)$  and  $85.49(5)^\circ$ ). These parameters are comparable to those observed for the homoleptic complex  $[(\text{F}_{12}\text{-Tp}^{4\text{Bo},3\text{Ph}})_2\text{Ca}]$ , even though the latter exhibits one inverted indazolyl ring.<sup>[31]</sup> Despite this distortion and the low coordination number, complex **1** does not show any agostic-type interaction involving the hexamethyldisilyl-amido group.

The Ca1–N7 bond (2.2342(15) Å) is shorter than the Ca–N<sub>amido</sub> bonds of related 4-coordinate complexes  $[\text{BDI}]\text{Ca}\{\text{N}(\text{SiMe}_3)_2\}(\text{thf})$ ,<sup>[33,34]</sup>  $[\text{N}^\wedge\text{N}]\text{Ca}\{\text{N}(\text{SiMe}_3)_2\}(\text{thf})$ ,<sup>[12,13]</sup> and  $[(\text{LX}_1)\text{Ca}\{\text{N}(\text{SiMe}_3)_2\}]$ <sup>[35]</sup> ( $\text{LX}_1 = \text{CH}_3\text{C}(\text{O}-2,6\text{-}i\text{Pr}_2\text{C}_6\text{H}_3\text{N})\text{CHC}(\text{CH}_3)(\text{NCH}_2\text{CH}_2\text{NMe}_2)$ ) (2.313(1), 2.286(3) and 2.303(4) Å, respectively). This can be ascribed to the presence of the electron-withdrawing fluorinated  $\{\text{F}_{12}\text{-Tp}^{4\text{Bo},3\text{Ph}}\}^-$  ligand in **1**.

Four-coordinate Ca complexes are not common. Only two four-coordinate Ca complexes bearing  $\kappa^3$ -N-bound ligands have been previously described: The alkoxide species  $[\text{Tp}^{\text{tBu}}\text{Ca}(\text{O}-2,6\text{-}i\text{Pr}_2\text{C}_6\text{H}_3)]$ , with the *t*Bu-substituted tris(pyrazolyl)borate ligand,<sup>[33,34]</sup> and the abovementioned  $[(\text{LX}_1)\text{Ca}\{\text{N}(\text{SiMe}_3)_2\}]$  complex, containing the tridentate  $\beta$ -diketiminato ligand  $\text{LX}_1$ .<sup>[35]</sup>

The one-pot procedure employed for the synthesis of several tris(pyrazolyl)borate Ca amido complexes<sup>[33]</sup> was not successful for the synthesis of **1**. Addition of THF or Et<sub>2</sub>O to a 1:1:1 mixture of [K(N(SiMe<sub>3</sub>)<sub>2</sub>), Ca], and [K(F<sub>12</sub>-Tp<sup>4Bo,3Ph</sup>)] provided the heteroleptic compounds [(F<sub>12</sub>-Tp<sup>4Bo,3Ph</sup>)Ca{N(SiMe<sub>3</sub>)<sub>2</sub>L<sub>x</sub>] in extremely low yields (L=THF, x=2, **1a**; L=Et<sub>2</sub>O, x=1, **1b**, 4% yield). Several byproducts either containing the {F<sub>12</sub>-Tp<sup>4Bo,3Ph</sup>} ligand or resulting from B–N bond cleavage were observed in all cases. After extraction with a 1:3 toluene/pentane mixture, compound **1a** yielded [(F<sub>12</sub>-Tp<sup>4Bo,3Ph</sup>)Ca{N(SiMe<sub>3</sub>)<sub>2</sub>}(thf)] (**1c**) in 7% yield. Attempts at crystallizing **1a** resulted in crystals of the indazolate complex [(F<sub>12</sub>-Tp<sup>4Bo,3Ph</sup>)Ca(3-PhIndF<sub>4</sub>)(thf)<sub>2</sub>] (**2**). The X-ray molecular structure of **2** (Figure 3) features two coord-

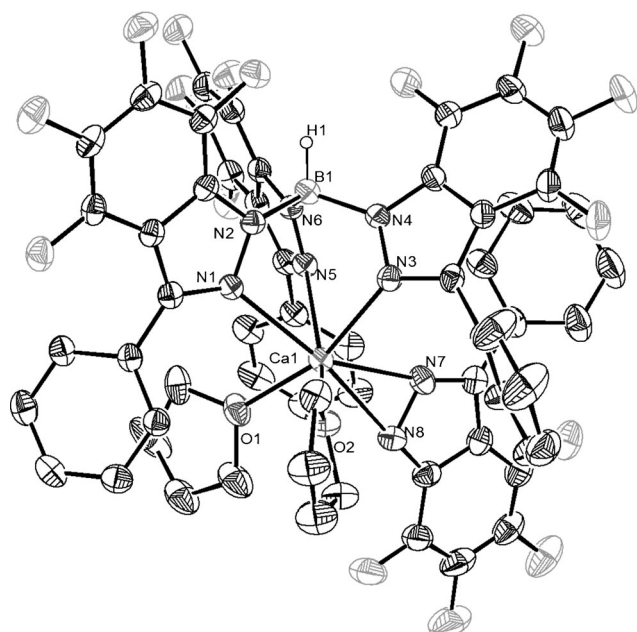


**Figure 3.** ORTEP drawing of [(F<sub>12</sub>-Tp<sup>4Bo,3Ph</sup>)Ca(3-PhIndF<sub>4</sub>)(thf)<sub>2</sub>] (**2**). Selected bond lengths [Å] and bond angles [°]: Ca1–N1 2.584(3), Ca1–N3 2.532(3), Ca1–N5 2.600(3), Ca1–N7 2.400(3), Ca1–N8 2.469(3); N1–Ca1–N5 75.78(8), N3–Ca1–N5 85.24(9), N3–Ca1–N1 76.69(8), N7–Ca1–N8 32.39(9), N7–Ca1–N3 83.30(9), N7–Ca1–N5 88.55(9), N7–Ca1–N1 155.40(10), N8–Ca1–N3 110.10(9), N8–Ca1–N5 108.14(9), N8–Ca1–N1 172.16(9).

inated THF molecules and an η<sup>2</sup>-indazolate ligand<sup>[36]</sup> arising from fragmentation of the [(F<sub>12</sub>-Tp<sup>4Bo,3Ph</sup>)] group by B–N bond cleavage. The 3-phenylindazolate ligand directs its phenyl group *syn* to the boron of {F<sub>12</sub>-Tp<sup>4Bo,3Ph</sup>} with Ca–N7 (2.400(3) Å) significantly shorter than Ca–N8 (2.469(3) Å). Coordination-induced B–N bond cleavage of tris(pyrazolyl)borates<sup>[37]</sup> and hydrobis- and tris-(imidazol-2-ylidene-1-yl)borates<sup>[23,24]</sup> have been observed previously. C–N bond cleavage in a tris(3-phenylpyrazolyl)methanide complex of calcium has also been reported.<sup>[38]</sup>

The strontium analogue of **1** has also been similarly synthesized. [(F<sub>12</sub>-Tp<sup>4Bo,3Ph</sup>)Sr{N(SiMe<sub>3</sub>)<sub>2</sub>}] (**3**) was isolated in 25% yield upon reaction of [Tl(F<sub>12</sub>-Tp<sup>4Bo,3Ph</sup>)] with an excess of [Sr{N(SiMe<sub>3</sub>)<sub>2</sub>}<sub>2</sub>] in pentane (Scheme 3). The <sup>1</sup>H and <sup>19</sup>F NMR spectra for **3** are qualitatively similar to those for **1**. A single

<sup>1</sup>H NMR resonance for the Si–CH<sub>3</sub> groups was observed at all temperatures between 298 and 183 K in [D<sub>8</sub>]toluene. An X-ray crystal structure has been obtained for **3** for which an ORTEP drawing is given in Figure 4 along with selected bond lengths

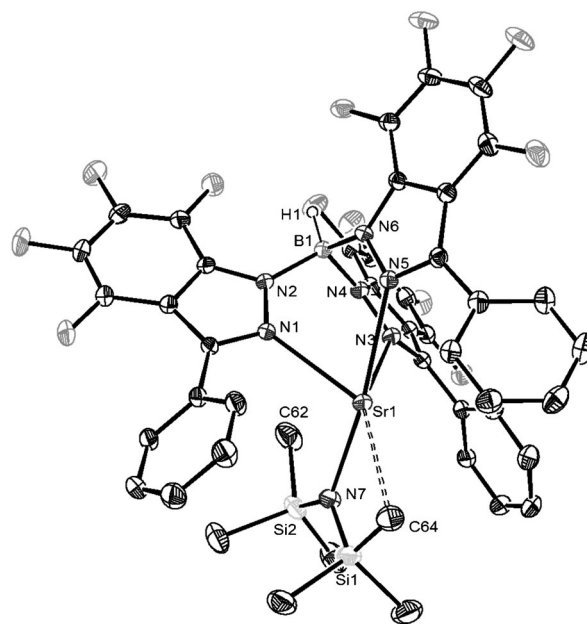


**Figure 4.** ORTEP drawing of [(F<sub>12</sub>-Tp<sup>4Bo,3Ph</sup>)Sr{N(SiMe<sub>3</sub>)<sub>2</sub>}] (**3**). Selected bond lengths [Å] and bond angles [°]: Sr1–N7 2.4219(18), Sr1–N1 2.6129(16), Sr1–N3 2.5784(16), Sr1–N5 2.7629(16); N7–Sr1–N1 104.69(6), N7–Sr1–N3 106.91(6), N7–Sr1–N5 166.96(6), N1–Sr1–N3 78.20(5), N3–Sr1–N5 62.36(5), N1–Sr1–N5 66.97(5).

and angles. Complex **3** has a monomeric structure and the metal center is only four-coordinate, a truly remarkable feature for such a large metal as strontium. Only two heteroleptic four-coordinate Sr amido complexes have been previously described: The [(BDI)Sr{N(SiMe<sub>3</sub>)<sub>2</sub>}(thf)]<sup>[39]</sup> and the [(N<sup>^</sup>N)Sr{N(SiMe<sub>3</sub>)<sub>2</sub>}(thf)]<sup>[13]</sup> amides, containing the κ<sup>2</sup>-N-bound β-diketiminate and imino-anilide ligand, respectively. Compound **3** is therefore the first heteroleptic four-coordinate Sr complex bearing a tripodal κ<sup>3</sup>-N-bound ligand. Unlike the Ca analogue **1**, the coordination sphere in **3** is strongly distorted and the geometry around Sr is best described as a trigonal bipyramid with a seemingly vacant equatorial coordination site (Figure 5). N5, one of the indazolyl nitrogen, and N7, the amido nitrogen, occupy the apical positions (N7–Sr1–N5 166.96(6)°), and N1 and N3 define two of the equatorial sites. Remarkably, the vacant equatorial site is occupied by one of the CH<sub>3</sub> groups of the {N(SiMe<sub>3</sub>)<sub>2</sub>} ligand suggesting that an agostic distortion is present in **3**. The two Sr–N–Si angles in **3** are indeed quite different with Sr1–N7–Si1 (106.84(10)°) being significantly less obtuse than Sr1–N7–Si2 (126.74(10)°). The distance Sr1...C64 (2.996(3) Å) is slightly longer than the sum of the covalent radii of Sr and C (2.71 Å)<sup>[40]</sup> and is significantly shorter than Sr1...C62 (ca., 3.81 Å). A similar barium complex of formula [(Tp<sup>Me2</sup>)Ba{N(SiMe<sub>3</sub>)<sub>2</sub>}(thf)<sub>2</sub>] has been also described.<sup>[41]</sup> It shows the favored κ<sup>3</sup>(N,N,N) coordination mode of the Tp ligand and

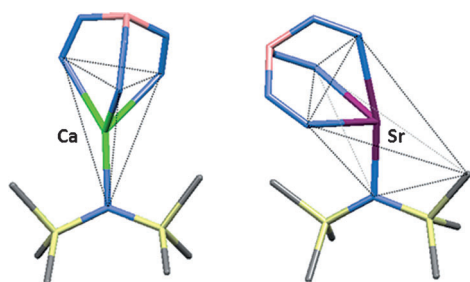


**Figure 5.** Different geometrical environments for complexes **1** (left) and **3** (right) highlighting the coordination polyhedra (distorted tetrahedron versus trigonal bipyramid, respectively) in shaded gray.

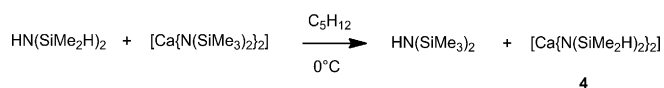
differently from compound **3**, it is six-fold coordinated with two molecules of THF completing the coordination sphere of the barium center.

Other Sr complexes featuring an asymmetrical arrangement of the  $\{N(SiMe_3)_2\}^-$  ligand have been previously described,<sup>[23,39,42–44]</sup> although the difference between the two Sr–N–Si angles is in all cases smaller than that observed in **3**. The Sr1–N5 bond *trans* to the amido is significantly longer (2.7629(16) Å) than Sr1–N1 and Sr1–N3 (2.6129(16) and 2.5784(16) Å), those two being in a range typical of  $[Tp'_2Sr]$  complexes.<sup>[45,46]</sup> The Sr1–N7 bond (2.4219(18) Å) is slightly shorter than the related bond length reported for the four-coordinate complexes  $\{[BDI]Sr\{N(SiMe_3)_2\}(thf)\}^{[39]}$  and  $\{[N^{\wedge}N]Sr\{N(SiMe_3)_2\}(thf)\}^{[13]}$  (2.446(2) and 2.463(2) Å, respectively), outlining the electron-withdrawing properties of the fluorinated  $\{F_{12}Tp^{4Bo,3Ph}\}^-$  ligand.

#### Synthesis and characterization of bis(dimethylsilylamido) calcium complexes $\{[LX]Ca\{N(SiMe_2H)_2\}\}$ ( $[LX] = N(SiMe_2H)_2, F_{12}Tp^{4Bo,3Ph}$ )

As reported for lanthanides<sup>[47–51]</sup> and Ae complexes,<sup>[52]</sup> the replacement of  $\{N(SiMe_3)_2\}^-$  by  $\{N(SiMe_2H)_2\}^-$  can impart a stabilizing effect by the formation of internal  $\beta$ -Si–H agostic interactions. Whereas  $[Ca\{N(SiMe_2H)_2\}_2(thf)]$  was known, its THF-free analogue  $[Ca\{N(SiMe_2H)_2\}_2]$  (**4**), a potentially very attractive starting material for Ca chemistry, was not. We first describe the synthesis and properties of **4** before presenting those of  $\{[F_{12}Tp^{4Bo,3Ph}]Ca\{N(SiMe_2H)_2\}\}$  (**5**).

Following a similar procedure to that used for the synthesis of  $[Ca\{N(SiMe_2H)_2\}_2(thf)]$ ,<sup>[52]</sup> transamination between  $HN(SiMe_2H)_2$  and  $[Ca\{N(SiMe_3)_2\}_2]$ <sup>[53–55]</sup> in pentane at 0 °C yielded the pure homoleptic  $[Ca\{N(SiMe_2H)_2\}_2]$  (**4**) in 87% yield (Scheme 4). Compound **4** is a highly air and moisture-sensitive white solid for which satisfactory elemental analyses were obtained. Despite numerous attempts, we were unable to crystallize **4**.



**Scheme 4.** Synthesis of  $[Ca\{N(SiMe_2H)_2\}_2]$  **4**.

Compound **4** is fluxional as revealed by a variable-temperature  $^1H$  NMR spectroscopic study in the 358–183 K range (Figure 6). According to this dynamic process, we propose that complex **4** is a trinuclear Ca species of the type  $[Ca\{N(SiMe_2H)_2\}_3]$ , displaying a linear array of three calcium atoms, bridged by four  $\{N(SiMe_2H)_2\}^-$  units and framed by two terminal symmetrical  $\{N(SiMe_2H)_2\}^-$  ligands as depicted in Figure 7. For comparison purposes, the diffusion coefficients of **4** and  $[Ca\{N(SiMe_3)_2\}_2]$  were measured by using DOSY NMR spectra in  $[D_8]toluene$  at 298 K. The values obtained ( $D_t = 0.6 \times 10^{-9}$  and  $1.0 \times 10^{-9} m^2 s^{-1}$  for **4** and  $[Ca\{N(SiMe_3)_2\}_2]$ , respectively) indicate that **4** has a higher nuclearity than  $[Ca\{N(SiMe_3)_2\}_2]$ . A diffusion molecular weight analysis against a series of reference compounds (D-fw) yielded a molecular weight of  $906 g mol^{-1}$  fully consistent with the trinuclear structure ( $913 g mol^{-1}$ ) proposed for **4** (see the Supporting Information).

In the fast exchange limit (358 K, Figure 6), two resonances for the SiH and the SiCH<sub>3</sub> groups were observed at  $\delta = 4.48$  and 0.37 ppm, respectively (1:6 ratio, label A''). A first exchange

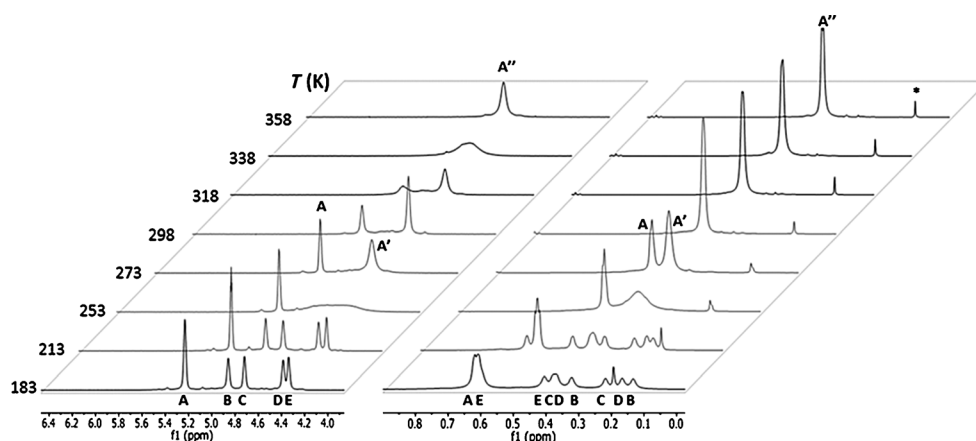


**Figure 6.** Variable-temperature  $^1H$  NMR spectra of **4** in  $[D_8]toluene$ . Low field enlargement = SiH region; high field enlargement = SiCH<sub>3</sub> region. \* = residual  $HN(SiMe_2H)_2$ .

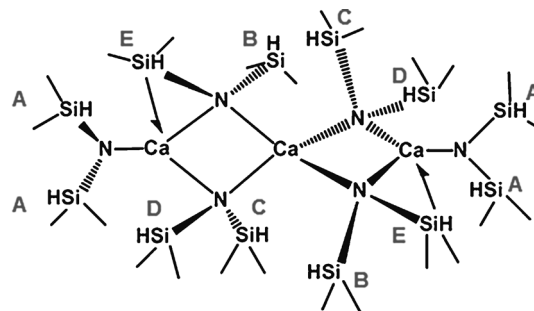


**Figure 7.** Schematic view of the proposed trinuclear structure for  $[Ca\{N(SiMe_2H)_2\}_3]$  (**4**) with labels according to the NMR spectra.

process was revealed upon cooling the sample below 338 K in which each of the SiH and SiCH<sub>3</sub> split to give each two resonances (A and A', Figure 6) in a 1:2 ratio ( $\Delta G^{\ddagger}_{330} \approx 69 \text{ kJ mol}^{-1}$ ).<sup>[56]</sup> Upon further cooling, line-broadening occurred only for each of the more shielded signals A' characterizing a second exchange process; below 253 K, the A' signals of the SiH and SiCH<sub>3</sub> groups split into four and eight separate resonances (B–E, Figure 6), respectively ( $\Delta G^{\ddagger}_{253} \approx 40 \text{ kJ mol}^{-1}$ ).<sup>[57]</sup> In the slow exchange limit (183 K), the <sup>1</sup>H NMR spectrum showed five types of SiMe<sub>2</sub>H signals, (A and B–E, Figure 6) in a 2:1:1:1:1 ratio. They correspond to five inequivalent SiMe<sub>2</sub>H groups, likely dependent on the presence of different β-Si–H agostic interactions with Ca.

Evidence for β-Si–H agostic interactions in **4** came from a <sup>1</sup>H-<sup>29</sup>Si HMQC 2D NMR experiment at 183 K. Figure 8 shows the correlations between five different <sup>29</sup>Si signals at  $\delta = -23.7$ ,

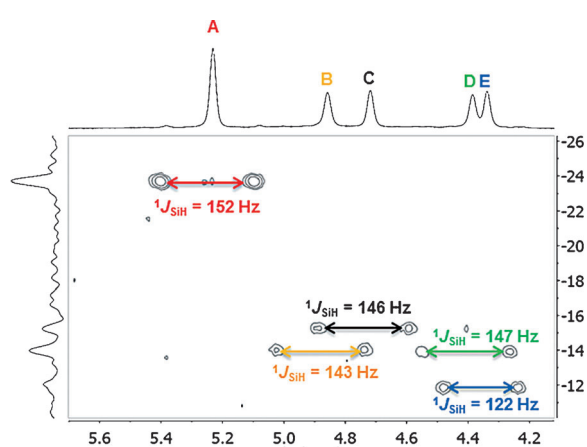


**Figure 8.** Si–H region enlargement of the <sup>1</sup>H-<sup>29</sup>Si HMQC 2D spectrum of **4** in [D<sub>8</sub>]toluene at 183 K.

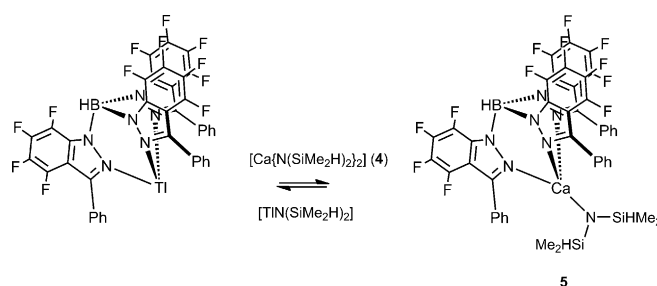
–15.3, –14.0, –13.9, and –11.8 ppm and the H<sub>A</sub>, H<sub>C</sub>, H<sub>B</sub>, H<sub>D</sub>, and H<sub>E</sub> protons, respectively (<sup>1</sup>J<sub>SiH</sub> = 152, 146, 143, 147, and 122 Hz, respectively). <sup>1</sup>J<sub>SiH</sub> coupling constants in the range 140–160 Hz suggest mild agostic interactions.<sup>[52,58]</sup> For SiH<sub>E</sub>, a stronger Ca...β-Si–H interaction is reflected by the lower <sup>1</sup>J<sub>SiH</sub> value of 122 Hz.<sup>[52,59,60]</sup> The presence of Si–H agostic interactions was further corroborated by solid-state IR spectroscopy: Whereas  $\nu_{\text{SiH}}$  of HN(SiMe<sub>2</sub>H)<sub>2</sub> is found at 2122 cm<sup>-1</sup>, three  $\nu_{\text{SiH}}$  absorptions are observed for **4** in the region 1900 to 2030 cm<sup>-1</sup>. The lowest  $\nu_{\text{SiH}}$  at 1905 cm<sup>-1</sup>, significantly lower than that for [Ca{N(SiMe<sub>2</sub>H)<sub>2</sub>}(thf)]<sub>2</sub>,<sup>[52]</sup> most likely reflects a stronger Ca...β-Si–H interaction. The presence of three  $\nu_{\text{SiH}}$  frequencies in the Si–H stretching modes region has been also reported for homoleptic TMEDA- or THF-coordinated Ca complexes containing the {C(SiMe<sub>2</sub>H)<sub>2</sub>}<sup>-</sup> ligand.<sup>[60]</sup>

Overall, exchange of terminal and bridging amido groups in **4** affords a single set of resonances in the fast exchange limit (A', Figure 6). By decreasing the temperature, the resonances for the terminal and bridging groups of the {N(SiMe<sub>2</sub>H)<sub>2</sub>}<sup>-</sup> ligands split into two signals in a 1:2 ratio (A and A'). At lower temperature, finally, the separation of the bridging SiH and SiCH<sub>3</sub> signals (A') into four well-defined peaks with a ratio

1:1:1:1 (B–E) reflects the four different types of bridging {N(SiMe<sub>2</sub>H)<sub>2</sub>}<sup>-</sup> groups with significant β-Si–H agostic interactions for the E sites (Figure 7). From the NMR spectroscopic data, there is no way to assign which resonance corresponds to the non-equivalent B, C, and D sites in Figure 7.

With the exception of the agostic interactions, the only previous example of a trinuclear homoleptic Ca complex is [Ca<sub>3</sub>(tBu<sub>2</sub>pz)<sub>6</sub>],<sup>[61]</sup> which exhibits a similar variable-temperature <sup>1</sup>H NMR behavior. Trinuclear homoleptic Mg compounds displaying two different ligand environments in a 1:2 ratio for the terminal and bridging positions are more common.<sup>[62–65]</sup> Trinuclear divalent lanthanide complexes of composition Ln{[μ-N(SiHMe<sub>2</sub>)<sub>2</sub>]<sub>2</sub>Ln[N(SiHMe<sub>2</sub>)<sub>2</sub>](thf)}<sub>2</sub> (Ln = Sm,<sup>[66]</sup> Yb,<sup>[67]</sup> and Eu<sup>[68]</sup>) have been also described. As in the case of complex **4**, the coordinatively unsaturated and electron-deficient Ln(II) centers favor the formation of close Ln...β-Si–H agostic interactions involving all of the SiHMe<sub>2</sub> groups. Extensive Eu...β-Si–H secondary interactions, finally, have been also reported very recently for the donor-free, mixed-valence, trinuclear complex Eu<sup>II</sup>{[μ-N(SiHMe<sub>2</sub>)<sub>2</sub>]<sub>2</sub>Eu<sup>III</sup>[N(SiHMe<sub>2</sub>)<sub>2</sub>]}<sub>3</sub>.<sup>[68]</sup>

Complex **4** has been used as a precursor for the synthesis of the heteroleptic compound [(F<sub>12</sub>-Tp<sup>4Bo,3Ph</sup>)Ca{N(SiMe<sub>2</sub>H)<sub>2</sub>}] (**5**). Treatment of [Ti(F<sub>12</sub>-Tp<sup>4Bo,3Ph</sup>)] with an excess of **4** in pentane over a period of 2 days, followed by extraction with a 1:3 toluene/pentane mixture, provided **5** in 37% yield (Scheme 5).



**Scheme 5.** Synthesis of complex **5**.

Compound **5** was characterized by elemental analysis, NMR, and IR spectroscopies. In the <sup>1</sup>H NMR spectrum at 298 K, the SiH resonance of **5** ( $\delta = 4.17 \text{ ppm}$ ) is significantly upfield with respect to the free amine ( $\delta = 4.92 \text{ ppm}$ ). In the <sup>1</sup>H-<sup>29</sup>Si HMQC 2D NMR spectrum, the SiH resonance is observed at  $\delta = -24.1 \text{ ppm}$  as a doublet with <sup>1</sup>J<sub>SiH</sub> = 159 Hz. As observed above for **4**, this time-average value is indicative of a mild (140–160 Hz) to weak (160–170 Hz) agostic interaction.<sup>[52][58]</sup> No decoalescence of the SiH signal was observed by variable-temperature <sup>1</sup>H NMR from 298 to 193 K in [D<sub>8</sub>]toluene. The solid-state IR data confirmed the presence of a β-Si–H agostic interaction. Compound **5** exhibited one  $\nu_{\text{SiH}}$  absorption at 2044 cm<sup>-1</sup> and a second remarkably low band at 1888 cm<sup>-1</sup>, characteristic of substantial Ca...β-Si–H interaction.

The solid-state structure of **5** was determined by X-ray diffraction (Figure 9). The metal center is four-coordinate, an uncommon feature for Ca complexes, with a short Ca–N<sub>amido</sub> distance (Ca–N7 = 2.261(2) Å), barely longer than that of **1**. Ex-

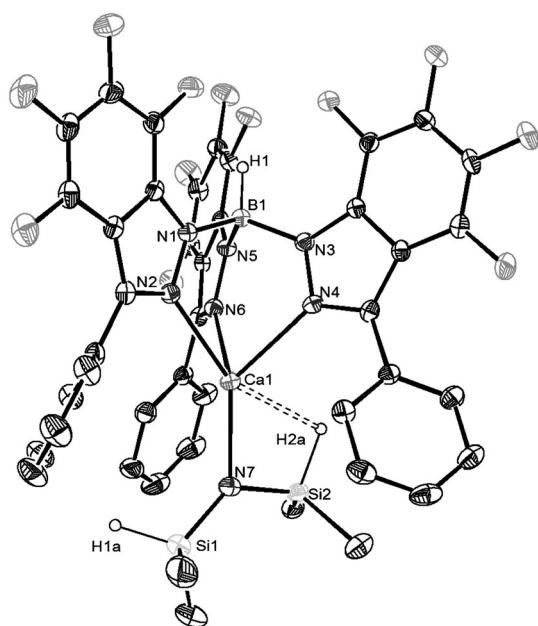


**Figure 9.** ORTEP drawing of  $[(F_{12}\text{-Tp}^{4Bo,3Ph})\text{Ca}\{N(\text{SiMe}_2\text{H})_2\}]$  **5**. Selected bond lengths [Å] and bond angles [°]: Ca1–N7 2.261(2), Ca1–N2 2.481(2), Ca1–N4 2.474(2), Ca1–N6 2.458(2) Ca1–H2a 2.41(2); N7–Ca1–N2 141.26(8), N7–Ca1–N4 133.31(8), N7–Ca1–N6 125.26(8), N2–Ca1–N4 75.97(7), N2–Ca1–N6 75.80(7), N4–Ca1–N6 82.40(7).

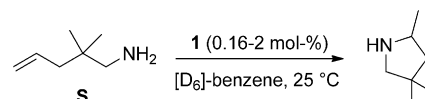
amination of the  $\text{Ca}\{N(\text{SiMe}_2\text{H})_2\}$  fragment strongly supports the presence of an agostic  $\text{Ca}\cdots\beta\text{-Si-H}$  contact, as the two  $\text{SiMe}_2\text{H}$  moieties are clearly non-equivalent. This is reflected by the difference between the obtuse Ca1–N7–Si1 and much more acute Ca1–N7–Si2 angles (134.99(13) and 97.92(10)°, respectively), corresponding to a much shorter Ca1 $\cdots$ Si2 distance (3.0003(9) Å) with respect to Ca1 $\cdots$ Si1 (3.655(1) Å). Interestingly, the agostic hydrogen H2a has been unambiguously localized (Ca1 $\cdots$ H2a = 2.41(2) Å), affording a nearly planar Ca1N7Si2H2a core (torsion angle 6.5°). Similar geometric features have been noted for other heteroleptic silylamido<sup>[69]</sup> and tris(dimethylsilyl)methyl<sup>[60,70]</sup> Ca complexes that also exhibit  $\beta\text{-Si-H}$  agostic interactions. The presence of this interaction is likely to confer a certain degree of stability, since **5** appeared significantly less reactive towards air and moisture than **1**.

Attempts at synthesizing the THF adduct of **5** were less successful. The treatment of  $[\text{Ti}(F_{12}\text{-Tp}^{4Bo,3Ph})]$  with  $[\text{Ca}\{N(\text{SiMe}_2\text{H})_2\}_2(\text{thf})]$  in pentane over a period of 2 days provided, after extraction with a 1:3 toluene/pentane mixture,  $[(F_{12}\text{-Tp}^{4Bo,3Ph})\text{Ca}\{N(\text{SiMe}_2\text{H})_2\}(\text{thf})]$  (**6**) as the major compound in 36% yield. Despite numerous attempts, it proved impossible to fully purify and analytically characterize **6**; crystals of **6** suitable for X-ray diffraction could not be obtained. In addition to **6**,  $^1\text{H}$  and  $^{19}\text{F}$  NMR spectroscopies revealed the presence of several unidentified species containing  $\{F_{12}\text{-Tp}^{4Bo,3Ph}\}^-$ . The  $^{19}\text{F}$  NMR spectrum of **6** (and the other species) shows four signals for the benzo fluorines of  $\{F_{12}\text{-Tp}^{4Bo,3Ph}\}^-$ . The  $^1\text{H}$  NMR spectrum of **6** shows SiH and SiCH<sub>3</sub> resonances at  $\delta = 4.69$  and 0.01 ppm, respectively, as well as THF signals whose integration is in accord with a mono adduct. In the  $^1\text{H}$ - $^{29}\text{Si}$  HMQC 2D NMR spectrum, the Si–H resonance is observed at  $\delta =$

–24.1 ppm with  $^1J_{\text{SiH}} = 160$  Hz. Addition of some drops of THF to a  $[D_6]$ benzene solution of **5** led to similar spectra and behavior.

### Cyclohydroamination catalysis

Our efforts towards the synthesis of **1** were rewarded upon examination of its catalytic performance for the cyclohydroamination of 1-amino-2,2-dimethyl-4-pentene (**S**) (Scheme 6), a common model aminoalkene for which abundant data are available in the literature. Representative results are gathered in Table 1.



**Scheme 6.** Cyclohydroamination reaction of **S** catalyzed by **1**.

**Table 1.** Representative data for the cyclohydroamination of **S** catalyzed by **1** at 25 °C.

| Entry            | [1]/[S] | t [min] | Conversion [%] <sup>[d]</sup> |
|------------------|---------|---------|-------------------------------|
| 1 <sup>[a]</sup> | 1:50    | 6       | 99                            |
| 2 <sup>[a]</sup> | 1:200   | 16      | 99                            |
| 3 <sup>[b]</sup> | 1:400   | 27      | 85                            |
| 4 <sup>[c]</sup> | 1:600   | 18      | 57                            |

[a] Reaction conditions: 3.0  $\mu\text{mol}$  of precatalyst, 1.2 mL of  $[D_6]$ benzene. [b] Reaction conditions: 3.0  $\mu\text{mol}$  of precatalyst, 1.8 mL of  $[D_6]$ benzene. [c] Reaction conditions: 3.0  $\mu\text{mol}$  of precatalyst, 1.7 mL of  $[D_6]$ benzene. [d] The conversions were determined by  $^1\text{H}$  NMR spectroscopic monitoring

In all cases, the ring-closure of **S** proceeded according to Baldwin's rules (5-*exo*-trig) leading to the exclusive formation of 2,4,4-trimethylpyrrolidine. Virtually complete conversion of 50 and 200 equivalents of **S** was observed within 6 and 16 min, respectively, at room temperature (turnover number, TON = 50 and 200; apparent turnover frequency,  $\text{TOF}_{\text{app}} = 8$  and  $12 \text{ min}^{-1}$ ). This reactivity highlights the highly effective catalytic activity of **1**, which, although comparable with the  $[\text{N}(\text{N})\text{Ca}(\text{X})(\text{thf})]$  systems ( $\text{X} = \text{N}(\text{SiMe}_3)_2$  or  $\text{CH}(\text{SiMe}_3)_2$ ),<sup>[13]</sup> outperforms that of the homoleptic complexes  $[\text{Ca}\{N(\text{SiMe}_3)_2(\text{thf})\}_x]$  ( $x = 0$  or 2) or  $[\text{Ca}\{\text{CH}(\text{SiMe}_3)_2(\text{thf})\}_2]$ ,<sup>[15]</sup> as well as that of the heteroleptic bis(imidazolin-2-ylidene-1-yl)borate-,<sup>[23]</sup> amino-phenolate-,<sup>[22]</sup> aminotroponimate-,<sup>[16]</sup> pyrrolyl-,<sup>[18]</sup> and  $\beta$ -diketimate-based<sup>[14,15]</sup> amido species. Therefore, compound **1** represents one of the most efficient precatalysts reported to date for the cyclohydroamination of **S**. When large loadings of 400 and 600 equivalents of aminoalkene were used, the conversion peaked at 85 and 57% after 27 and 18 min, respectively (TON = 340 and 342,  $\text{TOF}_{\text{app}} = 12$  and  $19 \text{ min}^{-1}$ ).

These results were found quite reproducible and can be ascribed to catalyst decomposition, consistently with the observed formation of an unidentified white precipitate during

the catalytic runs. Such catalyst decay at higher substrate loadings may be due to either the very high sensitivity of these Ae species towards residual impurities (moisture or other unidentified factors) contained in the substrate/solvent or intrinsic decomposition pathways of complex **1** (or species derived thereof) under the catalytic conditions. Kinetic monitoring was performed by  $^1\text{H}$  NMR spectroscopy at  $0^\circ\text{C}$  since at  $25^\circ\text{C}$  complex **1** was found too active for reliable measurements. Substrate consumption followed first-order kinetics; no induction period was observed (Figure 10). The semi-logarithmic plots of

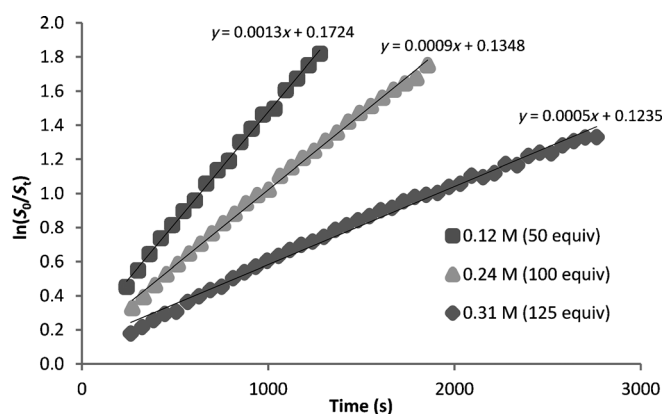


**Figure 10.** Semilogarithmic plot of substrate conversion versus reaction time for the cyclohydroamination of **S** (0.12, 0.24, and 0.31 M) catalyzed by **1**. Reaction conditions:  $0^\circ\text{C}$ ,  $3.0\ \mu\text{mol}$  of precatalyst in  $[\text{D}_6]\text{toluene}$  (1.2 mL).

monomer conversion versus reaction time were linear over 3 half-lives, with the apparent rate constants  $k_{\text{app}}$  values ranging from  $0.0005$  to  $0.0013\ \text{s}^{-1}$  for 125 and 50 equivalents of **S**, respectively (with  $k_{\text{app}} = k[\mathbf{1}]$  expressed in  $\text{s}^{-1}$ , in which  $k$  is the reaction rate constant in  $\text{L mol}^{-1}\ \text{s}^{-1}$ , see below). The reaction rates decreased when higher substrate concentrations were used, pointing to a possible catalyst inhibition by the product.

First-order dependence upon substrate concentration has also been observed for other heavier Ae-based catalytic systems,<sup>[13,22]</sup> although reaction rates with zeroth-order in substrate<sup>[22]</sup> or inversely proportional to substrate concentration may also be possible.<sup>[14,15]</sup>

To determine the effect of the precatalyst concentration upon the reaction rate, the cyclohydroamination of **S** was performed at  $0^\circ\text{C}$  with initial concentrations  $[\mathbf{1}]_0$  varying from 3.60 to 7.14 mM. The linear plot of  $\ln(k_{\text{app}})$  versus  $\ln([\mathbf{1}]_0)$  had a slope of 1.05 suggesting first-order dependence upon precatalyst concentration (see the Supporting Information). Thus, the rate law for the cyclohydroamination of the aminoalkene **S** catalyzed by **1** is given in Equation (1).

$$r = k[\mathbf{1}][\mathbf{S}] \quad (1)$$

Catalytic systems based on heavier alkaline earth metals that feature such a kinetic rate law are uncommon. Examples include the imino-anilide Ba-amido, and -alkyl precatalysts.<sup>[13]</sup> The same rate law was also established for Mg-based precatalysts supported by tris(oxazolynyl)phenylborate<sup>[71]</sup> or

phenoxy-amine ligands.<sup>[72]</sup> This rate law is consistent with a mechanism implying a fast  $\sigma$ -insertive pathway followed by rate-limiting aminolysis, as recently computed for both intra- and intermolecular hydroamination.<sup>[73–75]</sup>

Alternatively, it may also be accounted for by the interaction between two substrate molecules and the metal center, with the formation of a six-membered transition state involving concerted ring-closure and proton transfer, as the turnover-limiting step.<sup>[71]</sup> DFT computations performed on  $\{\text{Cpo}^{\text{M}}\}\text{Y}^{\text{III}}$  alkyl,  $\{\text{To}^{\text{M}}\}\text{Mg}^{\text{II}}$  alkyl, and anilido-imine-Ae complexes suggested that the latter scenario may be significantly more energy demanding, and therefore less realistic ( $\{\text{Cpo}^{\text{M}}\}$  = cyclopentadienyl-bis(oxazolynyl)borate,  $\{\text{To}^{\text{M}}\}$  = tris(oxazolynyl)borate).<sup>[73–75]</sup>

The strontium analogue **3** was also evaluated in the intramolecular hydroamination reaction of **S**, displaying a much lower catalytic activity than its Ca analogue. The reaction with 50 equivalents of the aminoalkene at  $25^\circ\text{C}$  only provided a conversion of 10% in 7 min. Signs of catalyst decomposition were noted with also the formation of a white precipitate at the bottom of the NMR tube within seconds after the reactants were mixed. Apparently, the active species in the strontium case decomposes much faster than in the calcium case.<sup>[76]</sup>

## Conclusion

The synthesis and characterization of the silylamido complexes  $[(\text{F}_{12}\text{-Tp}^{4\text{Bo},3\text{Ph}})\text{Ae}(\text{NR}_2)]$  ( $\text{R} = \text{SiMe}_3$ ,  $\text{Ae} = \text{Ca}, \text{Sr}$ ;  $\text{R} = \text{SiMe}_2\text{H}$ ,  $\text{Ae} = \text{Ca}$ ) supported by the bulky, highly fluorinated, hydrotris(indazolyl)borate ligand  $\{\text{F}_{12}\text{-Tp}^{4\text{Bo},3\text{Ph}}\}^-$  have been detailed. These heteroleptic complexes, free of ethereal ligands, are inert in solution, showing a remarkable inertness towards Schlenk equilibria. The solid-state structure of  $[(\text{F}_{12}\text{-Tp}^{4\text{Bo},3\text{Ph}})\text{Sr}\{\text{N}(\text{SiMe}_3)_2\}]$  (**3**) displays an agostic interaction between the electron-deficient  $\text{Sr}^{2+}$  center and one of the Si–CH<sub>3</sub> groups of the  $\{\text{N}(\text{SiMe}_3)_2\}^-$  ligand. The synthesis of the new homoleptic diamido complex  $[\text{Ca}\{\text{N}(\text{SiMe}_2\text{H})_2\}_2]$  (**4**) has been described. On the basis of its fluxional behavior, a trinuclear structure with additional  $\beta$ -Si–H agostic interactions has been proposed for **4**. This precursor has enabled the synthesis of the heteroleptic THF-free compound  $[(\text{F}_{12}\text{-Tp}^{4\text{Bo},3\text{Ph}})\text{Ca}\{\text{N}(\text{SiMe}_2\text{H})\}]$  **5**, also stabilized by a  $\beta$ -Si–H agostic contact.

Complex **1** proved to be particularly efficient for the catalytic cyclohydroamination of 1-amino-2,2-dimethyl-4-pentene, representing one of the most active precatalysts reported to date for this reaction. However, the activity of **1** seems limited by catalyst degradation over time with large substrate loadings (much higher than those reported in the literature), a feature apparently even more obvious for the strontium analogue **3**.

Despite stability issues largely due to B–N bond cleavage, the highly fluorinated ligand  $\{\text{F}_{12}\text{-Tp}^{4\text{Bo},3\text{Ph}}\}^-$  forms well-defined heteroleptic Ca and Sr silylamido complexes. Its electron-withdrawing properties coupled to the bulky tripodal scaffold enhance the polarity and hence the reactivity of the Ae–N bond yet avoiding Schlenk-type redistributions. This is remarkable since there are only very few ligands capable of preventing scrambling equilibria during catalysis, especially in the case of Sr.<sup>[12,13]</sup>

## Experimental Section

All operations were performed with rigorous exclusion of air and moisture, using standard Schlenk, high-vacuum, and glovebox techniques under Ar ( $O_2 < 3$  ppm,  $H_2O < 1$  ppm). All solvents were dried and distilled under Ar (THF over Na/benzophenone; acetone over drierite; toluene over Na; pentane over  $CaH_2$ ) and further degassed by freeze–pump–thaw cycles. Deuterated solvents were dried over molecular sieves, filtered, and degassed by several freeze–pump–thaw cycles and stored in sealed ampules in the glovebox.  $[Ti(F_{12}\text{-Tp}^{4Bo,3Ph})]$  was prepared as previously reported.<sup>[28]</sup>  $Ca_2$  and  $SrI_2$  (Aldrich; anhydrous beads, –10 mesh, 99.999% trace metal basis) were used as received.  $HN(SiMe_2H)_2$  (97%) was dried over activated 3 Å molecular sieves.  $HN(SiMe_3)_2$  was distilled over  $CaH_2$ . The substrate 1-amino-2,2-dimethyl-4-pentene (**5**) was prepared according to literature methods.<sup>[77]</sup>  $KN(SiMe_3)_2$  was prepared from KH and  $HN(SiMe_3)_2$  following the same procedure used for  $KN(SiMe_2H)_2$ .<sup>[52]</sup>  $[Ca\{N(SiMe_3)_2\}_2]$  and  $[Sr\{N(SiMe_3)_2\}_2]$  were synthesized from  $KN(SiMe_3)_2$  and either  $Ca_2$  or  $SrI_2$  according to literature procedures.<sup>[78,79]</sup>  $[Ca\{N(SiMe_2H)_2\}_2(thf)]$  was prepared as previously reported.<sup>[52]</sup>

Unless stated otherwise, NMR spectra were recorded by using J. Young valve NMR tubes at 298 K using Bruker DPX 300 ( $^1H$ , 300.13;  $^{19}F$ , 282.38 MHz) Avance III 400 ( $^1H$ , 400.16;  $^{19}F$ , 376.49 MHz), Avance 300 ( $^1H$ , 300.13,  $^{19}F$ , 282.38 MHz), Avance 400 ( $^1H$ , 400.13;  $^{19}F$ , 376.48;  $^{13}C$ , 100.63 MHz), or Avance 500 ( $^1H$ , 500.33;  $^{29}Si$  79.49;  $^{13}C$  125.82 MHz) spectrometers. Chemical shifts for  $^1H$  NMR were determined using residual proton signals in the deuterated solvents and reported versus  $SiMe_4$ . Chemical shifts for  $^{13}C$  NMR spectra were that of the solvent referenced to  $SiMe_4$ .  $^{19}F$  and  $^{29}Si$  NMR spectra were referenced versus external  $CFCl_3$  and  $SiMe_4$ , respectively.  $^1H$ - $^{29}Si$  HMQC NMR experiments were carried out when needed. DOSY NMR experiments were carried out on a Bruker Avance 500 spectrometer equipped with a 5 mm triple resonance inverse Z-gradient probe (TBI $^1H$ ,  $^{31}P$ , BB). The DOSY spectra were acquired at 293 K with the steppgp1s pulse program from Bruker topspin software. All spectra were recorded with 16 K time domain data point in the t2 dimension and 16 t1 increments. The strength of the gradient was linearly incremented in 16 steps from 2 up to 95% of the maximum gradient strength. All measurements were performed with a compromise diffusion delay  $\Delta$  of 100 ms and a gradient pulse length  $\delta$  of 1.8 ms. Infrared spectra were performed on a PerkinElmer 100 FTIR spectrometer equipped with an ATR device for measurements in the solid state into a glovebox. Elemental analyses (London Metropolitan University or Analytical service of the LCC) are the average of at least two independent measurements.

**Synthesis of  $[(F_{12}\text{-Tp}^{4Bo,3Ph})Ca\{N(SiMe_3)_2\}]$  (1):**  $[Ti(F_{12}\text{-Tp}^{4Bo,3Ph})]$  (0.500 g, 0.494 mmol) and  $Ca\{N(SiMe_3)_2\}_2$  (0.414 g, 1.148 mmol) were combined in a flask and pentane (10 mL) was added. The resulting white slurry was stirred at room temperature for two days. After filtration and washing with pentane, the product was extracted with a toluene/pentane (1:3 v/v) mixture. After removal of volatiles under vacuum, compound **1** was obtained as a white solid (0.334 g, 67%). Crystals suitable for X-ray diffraction analysis were obtained from a saturated toluene/pentane solution of **1** at  $-40^\circ C$ .  $^1H$  NMR ( $[D_6]benzene$ ):  $\delta = 7.54$  (d,  $^3J_{HH} = 8.3$  Hz, 6H, *o*- $C_6H_5$ ), 7.32 (t,  $^3J_{HH} = 7.7$  Hz, 6H, *m*- $C_6H_5$ ), 7.23 (d,  $^3J_{HH} = 7.5$  Hz, 3H, *p*- $C_6H_5$ ),  $-0.34$  ppm (s, 18H,  $SiCH_3$ );  $^{19}F$  NMR ( $[D_6]benzene$ , 377 MHz):  $\delta = -144.30$  (t,  $J_{FF} = 18.1$  Hz, 3 F, *F-4*),  $-151.59$  (d,  $J_{FF} = 10.2$  Hz, 3 F, *F-6*),  $-153.83$  (t,  $J_{FF} = 17.6$  Hz, 3 F, *F-7*),  $-164.15$  ppm (t,  $J_{FF} = 20.7$  Hz, 3 F, *F-5*); elemental analysis calcd (%) for  $C_{45}H_{34}N_7BSi_2F_{12}Ca$ : C 53.62, H 3.38, N 9.73; found: C 53.42, H 3.21, N 9.56.

**One-pot synthesis of  $[(F_{12}\text{-Tp}^{4Bo,3Ph})Ca\{N(SiMe_3)_2\}(thf)_x]$  ( $x = 2$ , **1a**;  $x = 1$ , **1c**):**  $KN(SiMe_3)_2$  (0.068 g, 0.343 mmol),  $Ca_2$  (0.101 g, 0.343 mmol),  $K(F_{12}\text{-Tp}^{4Bo,3Ph})$  (0.290 g, 0.343 mmol), and THF (10 mL) were added to a Schlenk flask. The mixture was stirred at room temperature for 8 h. After removal of volatiles under vacuum, the resulting solid was washed with pentane, extracted with toluene and filtered, affording a solution of **1a**. After removal of volatiles under vacuum, the solid was washed with pentane and extracted into a toluene/pentane (1:3 v/v) mixture, affording **1c** in 7% yield. Compound **1c** decomposes in solution over a period of few hours. **Compound 1a:**  $^1H$  NMR ( $[D_6]benzene$ , 300 MHz):  $\delta = 7.81$  (dd,  $J_{HH} = 8.1$ , 3.0 Hz, 6H, *o*- $C_6H_5$ ), 7.27 (t,  $^3J_{HH} = 7.6$  Hz, 6H, *m*- $C_6H_5$ ), 2.89 (brm, 8H,  $OCH_2$ ), 0.81 (brm, 8H,  $CH_2$ ),  $-0.10$  ppm (s, 18H,  $SiCH_3$ );  $^{19}F$  NMR ( $[D_6]benzene$ , 282 MHz):  $\delta = -143.82$  (t,  $J_{FF} = 17.1$  Hz, 3 F, *F-4*),  $-151.32$  (s, 3 F, *F-6*),  $-154.39$  (m, 3 F, *F-7*),  $-164.14$  ppm (t,  $J_{FF} = 20.3$  Hz, 3 F, *F-5*); **1c**  $^1H$  NMR ( $[D_6]benzene$ , 300 MHz):  $\delta = 7.75$  (dd,  $J_{HH} = 8.3$ , 2.8 Hz, 6H, *o*- $C_6H_5$ ), 7.29 (t,  $^3J_{HH} = 7.6$  Hz, 6H, *m*- $C_6H_5$ ), 2.76 (br m, 4H,  $OCH_2$ ), 0.69 (brm, 4H,  $CH_2$ ),  $-0.15$  ppm (s, 18H,  $SiCH_3$ );  $^{19}F$  NMR ( $[D_6]benzene$ , 298 K, 282 MHz):  $\delta = -143.93$  (t,  $J_{FF} = 18.1$  Hz, 3 F, *F-4*),  $-151.37$  (s, 3F, *F-6*),  $-154.25$  (t,  $J_{FF} = 17.8$  Hz, 3 F, *F-7*),  $-164.14$  ppm (t,  $J_{FF} = 20.3$  Hz, 3 F, *F-5*).

**One-pot synthesis of  $[(F_{12}\text{-Tp}^{4Bo,3Ph})Ca\{N(SiMe_3)_2\}(Et_2O)]$  (1b):**  $KN(SiMe_3)_2$  (0.118 g, 0.590 mmol),  $Ca_2$  (0.174 g, 0.590 mmol),  $K(F_{12}\text{-Tp}^{4Bo,3Ph})$  (0.500 g, 0.590 mmol), and  $Et_2O$  (10 mL) were added to a Schlenk flask. The mixture was stirred at room temperature for 3 days. After removal of volatiles under vacuum, the resulting solid was washed with pentane, extracted with a toluene/pentane (1:3 v/v) mixture, and filtered. Removal of solvents afforded **1b** in 3% yield. **1b** decomposes in solution over a period of few hours.  $^1H$  NMR ( $[D_6]benzene$ , 400 MHz):  $\delta = 7.54$  (d,  $^3J_{HH} = 7.8$  Hz, 6H, *o*- $C_6H_5$ ), 7.31 (t,  $^3J_{HH} = 7.5$  Hz, 6H, *m*- $C_6H_5$ ), 7.22 (t,  $^3J_{HH} = 7.5$  Hz, 3H, *p*- $C_6H_5$ ), 3.17 (brm, 4H,  $OCH_2$ ), 1.02 (brm, 6H,  $CH_3$ ),  $-0.34$  ppm (s, 18H,  $SiCH_3$ );  $^{19}F$  NMR ( $[D_6]benzene$ , 376 MHz):  $\delta = -144.28$  (t,  $J_{FF} = 18.1$  Hz, 3 F, *F-4*),  $-151.58$  (m, 3 F, *F-6*),  $-153.78$  ppm (t,  $J_{FF} = 17.7$  Hz, 3 F, *F-7*);  $\delta = -164.09$  ppm (t,  $J_{FF} = 20.0$  Hz, 3 F, *F-5*).

**Synthesis of  $[(F_{12}\text{-Tp}^{4Bo,3Ph})Sr\{N(SiMe_3)_2\}]$  (3):**  $[Ti(F_{12}\text{-Tp}^{4Bo,3Ph})]$  (0.200 g, 0.198 mmol),  $[Sr\{N(SiMe_3)_2\}_2]$  (0.121 g, 0.297 mmol), and pentane (10 mL) were combined in a Schlenk flask. The white slurry was stirred at room temperature for 2 days. After filtration and washing with pentane, the solid was extracted with a toluene/pentane (1:3 v/v) mixture and filtered. After removal of volatiles under vacuum, compound **3** was obtained as a white solid (0.052 g, 25%, non-optimized yield). Crystals suitable for X-ray diffraction were obtained from a concentrated toluene/pentane solution at  $-40^\circ C$ .  $^1H$  NMR ( $[D_6]benzene$ , 300 MHz):  $\delta = 7.47$  (d,  $^3J_{HH} = 7.4$  Hz, 6H, *o*- $C_6H_5$ ), 7.30 (t,  $^3J_{HH} = 7.4$  Hz, 6H, *m*- $C_6H_5$ ), 7.21 (t,  $^3J_{HH} = 7.5$  Hz, 3H, *p*- $C_6H_5$ ),  $-0.34$  ppm (s, 18H,  $SiCH_3$ );  $^{19}F$  NMR ( $[D_6]benzene$ , 282 MHz):  $\delta = -144.60$  (t,  $J_{FF} = 18.3$  Hz, 3 F, *F-4*),  $-151.36$  (m, 3 F,  $J_{FF} = 11.0$  Hz, *F-6*),  $-154.33$  (t,  $J_{FF} = 18.0$  Hz, 3 F, *F-7*),  $-164.30$  ppm (t,  $J_{FF} = 20.1$  Hz, 4 F, *F-5*); elemental analysis calcd (%) for  $C_{45}H_{34}N_7BSi_2F_{12}Sr$ : C 51.20, H 3.22, N 9.29; found: C 51.06, H 3.11, N 9.20.

**Synthesis of  $[Ca\{N(SiMe_2H)_2\}_2]$  (4):**  $[Ca\{N(SiMe_3)_2\}_2]$  (0.410 g, 1.138 mmol) and pentane (20 mL) were added to a Schlenk flask and cooled down to  $0^\circ C$  in an ice–water bath.  $HN(SiMe_2H)_2$  (0.494 mL, 2.844 mmol) was then added dropwise with stirring for about 30 min. The solution was then stirred at  $0^\circ C$  for 2.5 h. After removal of volatiles under vacuum, pentane was added and stripped under vacuum to afford **4** as a white solid (0.300 g, 87%).  $^1H$  NMR ( $[D_6]benzene$ , 400 MHz):  $\delta = 5.07$  (s, SiH), 4.61 (s, SiH), 0.43 (s,  $SiCH_3$ ), 0.35 ppm (s,  $SiCH_3$ );  $^{13}C\{^1H\}$  NMR ( $[D_6]benzene$ , 125.82 MHz):  $\delta = 4.54$  (s,  $SiCH_3$ ), 4.06 ppm (s,  $SiCH_3$ );  $^1H$  NMR ( $[D_3]toluene$ , 183 K, 500 MHz):  $\delta = 5.25$  (s, 4H,  $SiH_A$ ), 4.88 (s, 2H,

SiH<sub>6</sub>), 4.74 (s, 2H, SiH<sub>C</sub>), 4.41 (s, 2H, SiH<sub>D</sub>), 4.36 (s, 2H, SiH<sub>E</sub>), 0.64 (s, 24H, SiCH<sub>3A</sub>), 0.61 (s, 6H, SiCH<sub>3E</sub>), 0.43 (s, 6H, SiCH<sub>3E</sub>), 0.39 (s, 6H, SiCH<sub>3C</sub>), 0.38 (s, 6H, SiCH<sub>3D</sub>), 0.34 (s, 6H, SiCH<sub>3B</sub>), 0.24 (s, 6H, SiCH<sub>3C</sub>), 0.18 (s, 6H, SiCH<sub>3D</sub>), 0.15 ppm (s, 6H, SiCH<sub>3B</sub>); <sup>1</sup>H-<sup>29</sup>Si HMQC 2D NMR ([D<sub>6</sub>]toluene, 183 K, 79.49 MHz): δ = 11.8 (d, <sup>1</sup>J<sub>SiH</sub> = 122 Hz, SiH<sub>E</sub>), -13.9 (d, <sup>1</sup>J<sub>SiH</sub> = 147 Hz, SiH<sub>D</sub>), -14.0 (d, <sup>1</sup>J<sub>SiH</sub> = 143 Hz, SiH<sub>B</sub>), -15.3 (d, <sup>1</sup>J<sub>SiH</sub> = 146 Hz, SiH<sub>C</sub>), -23.7 ppm (d, <sup>1</sup>J<sub>SiH</sub> = 152 Hz, SiH<sub>A</sub>); IR: ν<sub>SiH</sub> = 2032 (sh), 1957 (s), 1095 cm<sup>-1</sup> (sh); elemental analysis calcd (%) for C 31.5, H 9.2, N 9.2; found: C 31.25, H 9.37, N 9.22.

**Synthesis of [(F<sub>12</sub>-Tp<sup>4Bo,3Ph</sup>)Ca{N(SiMe<sub>2</sub>H)<sub>2</sub>}] (5):** [Ti(F<sub>12</sub>-Tp<sup>4Bo,3Ph</sup>)] (0.259 g, 0.256 mmol), Ca[N(SiMe<sub>2</sub>H)<sub>2</sub>]<sub>2</sub> (0.117 g, 0.384 mmol), and pentane (8 mL) were combined in a flask. The white slurry was stirred at room temperature for 2 days, during which time it changed color to dark gray. After filtration and washing with pentane, the solid was extracted with a toluene/pentane (1:3 v/v) mixture and filtered. After removal of volatiles under vacuum, compound **5** was obtained as a white solid (0.095 g, 37%, un-optimized yield). Crystals suitable for X-ray diffraction analysis were obtained from a saturated toluene/pentane solution at -40 °C. <sup>1</sup>H NMR ([D<sub>6</sub>]benzene, 400 MHz): δ = 7.48 (d, <sup>3</sup>J<sub>HH</sub> = 8.0 Hz, 6H, o-C<sub>6</sub>H<sub>5</sub>), 7.31 (t, 6H, <sup>3</sup>J<sub>HH</sub> = 7.6 Hz, m-C<sub>6</sub>H<sub>5</sub>), 7.21 (t, <sup>3</sup>J<sub>HH</sub> = 7.5 Hz, 3H, p-C<sub>6</sub>H<sub>5</sub>), 4.17 (br m, 2H, SiH), -0.23 ppm (d, <sup>3</sup>J<sub>HH</sub> = 2.8 Hz, 12H, SiCH<sub>3</sub>); <sup>19</sup>F NMR ([D<sub>6</sub>]benzene, 376 MHz): δ = -144.39 (t, J<sub>FF</sub> = 18.2 Hz, 3 F, F-4), -151.71 (d, J<sub>FF</sub> = 10.5 Hz, 3 F, F-6), -153.92 (t, J = 18.0 Hz, 3 F, F-7), -164.15 ppm (t, J = 20.1 Hz, 3 F, F-5); <sup>29</sup>Si NMR ([D<sub>6</sub>]benzene, 79.49 MHz): δ = -24.1 ppm (d, <sup>1</sup>J<sub>SiH</sub> = 159 Hz, SiH); IR: ν<sub>SiH</sub> = 2044 (s), 1888 cm<sup>-1</sup> (s); elemental analysis calcd (%) for C<sub>43</sub>H<sub>30</sub>N<sub>7</sub>BSi<sub>2</sub>F<sub>12</sub>Ca: C 52.70, H 3.06, N 10.01; found: C 52.59, H 3.25, N 9.92.

**Synthesis of [(F<sub>12</sub>-Tp<sup>4Bo,3Ph</sup>)Ca{N(SiMe<sub>2</sub>H)<sub>2</sub>}(thf)] (6):** [Ti(F<sub>12</sub>-Tp<sup>4Bo,3Ph</sup>)] (0.179 g, 0.177 mmol), [Ca{N(SiMe<sub>2</sub>H)<sub>2</sub>}(thf)] (0.100 g, 0.266 mmol) and pentane (8 mL) were combined in a flask. The white slurry was stirred at room temperature for 2 days during which time it changed color to dark gray. After filtration and washing with pentane, the solid was extracted with toluene/pentane (1:3 v/v) mixture. After removal of volatiles under vacuum, compound **6** was obtained as a white solid (0.060 g, 32%). <sup>1</sup>H NMR ([D<sub>6</sub>]benzene, 300 MHz): δ = 7.75 (d, <sup>3</sup>J<sub>HH</sub> = 7.4 Hz, 6H, o-C<sub>6</sub>H<sub>5</sub>), 7.31 (t, <sup>3</sup>J<sub>HH</sub> = 7.6 Hz, 6H, m-C<sub>6</sub>H<sub>5</sub>), 7.02 (d, <sup>3</sup>J<sub>HH</sub> = 6.7 Hz, 3H, p-C<sub>6</sub>H<sub>5</sub>), 4.69 (br m, 2H, SiH), 2.68 (t, 4H, OCH<sub>2</sub>), 0.70 (t, 4H, CH<sub>2</sub>), 0.01 ppm (d, <sup>3</sup>J<sub>SiH</sub> = 2.9 Hz, 12H, SiCH<sub>3</sub>); <sup>19</sup>F NMR ([D<sub>6</sub>]benzene, 282 MHz): δ = -143.58 (t, J<sub>FF</sub> = 18.1 Hz, 3 F, F-4), -151.43 (m, 3F, F-6), -154.56 (t, J<sub>FF</sub> = 17.4 Hz, 3 F, F-7), -164.40 ppm (t, J<sub>FF</sub> = 20.2 Hz, 3 F, F-5); <sup>29</sup>Si NMR ([D<sub>6</sub>]benzene, 79.49 MHz): δ = -24.1 ppm (d, <sup>1</sup>J<sub>SiH</sub> = 160 Hz, SiH); Satisfactory elemental analyses could not be obtained.

### NMR-scale cyclohydroamination reactions

In a glovebox, the appropriate amount of catalyst (**1** or **3**) was weighed in an NMR tube, and the substrate dissolved in [D<sub>6</sub>]benzene was then added. The tube was sealed, vigorously shaken, and immersed into an oil bath at the desired temperature. After the required amount of time, the NMR tube was removed from the oil bath and the <sup>1</sup>H NMR spectrum of the reaction mixture was recorded. The conversion was calculated by comparing the relative intensities of resonance signals characteristic of the substrate and product.

### Kinetics of the cyclohydroamination reaction

In a glovebox, the appropriate amount of precatalyst was weighed in an NMR tube. The substrate and [D<sub>6</sub>]toluene (1.6, 1.7, or 1.8 mL) were then added to the NMR tube. The tube was rapidly sealed and vigorously shaken, then cooled in a bath at 0 °C (reaction times were measured from this point) and maintained at this tem-

perature until it was inserted into the probe of a Bruker AM 500 NMR spectrometer preset at 0 °C. Data points were recorded as soon as possible after this, and it typically took altogether about 5 min to record the first of these. The reaction kinetics were monitored (using the multi zgvd command; D1 = 0.2 s; DS = 0; NS = 4 or more) over the course of 3 or more half-lives on the basis of amine consumption, by comparing the relative intensities of resonances diagnostic of substrate and product.

### X-ray diffraction crystallography

The data for crystals of **1** and **2** were collected on a Gemini Ultra diffractometer from Agilent equipped with an Oxford Instrument Cooler Device. Mirror monochromatized Cu<sub>Kα</sub> radiation was used for collecting diffraction data at a temperature of T = (180 ± 2) K. The data for crystals of **3** were collected on a Bruker D8 diffractometer equipped with APEX II detector and an Oxford Cryosystem N<sub>2</sub> gas stream low-temperature device. Graphite-monochromatized Mo<sub>Kα</sub> radiation was used for collecting diffraction data at a temperature of T = (180 ± 2) K. The data for crystals of **5** were collected on a Bruker D8 diffractometer equipped with APEX II detector and an Oxford Cryosystem N<sub>2</sub> gas stream low-temperature device. Multi-layer-monochromatized micro-focus Mo<sub>Kα</sub> radiation was used for collecting diffraction data at a temperature of T = (193 ± 2) K. The structure was solved by direct methods using SIR92<sup>[80]</sup> and refined by means of least-squares procedures on F<sup>2</sup> with the aid of the program SHELX-L97<sup>[81]</sup> included in the software package WinGX version 1.63.<sup>[82]</sup> All non-hydrogen atoms were anisotropically refined. All hydrogen atoms were geometrically placed and refined by using a riding model. In the last cycles of refinement a weighting scheme was used, where weights were calculated from the following formula: w = 1/[σ<sup>2</sup>(Fo<sup>2</sup>) + (0.0380P)<sup>2</sup> + 1.1258P] in which P = (Fo<sup>2</sup> + 2Fc<sup>2</sup>)/3. For complex **2**, a disorder between two molecules of THF was treated using the PART command in SHELX-L97. For complex **2**, the checkcif presents one Alert level A about a low theta full: The reason is due to incomplete scans, possibly based on erroneously assumed higher than actual symmetry for the final measurement strategy determination. Ellipsoids were drawn at the 30% probability level. Relevant collection and refinement data are summarized in the Supporting Information.

CCDC-1025065 (**1**), CCDC-1025066 (**2**), CCDC-1025067 (**3**), and CCDC-1025068 (**5**) contain the supplementary crystallographic data for this paper. These data can be obtained free of charge from The Cambridge Crystallographic Data Centre via [www.ccdc.cam.ac.uk/data\\_request/cif](http://www.ccdc.cam.ac.uk/data_request/cif).

### Acknowledgements

Financial support from the ANR (GreenLAKE project; contract number ANR-11-BS07-0009) is gratefully acknowledged. The assistance of Dr. Remy Brousses with the X-ray diffraction crystallography and Dr. Christian Bijani with the NMR spectroscopy measurements is also acknowledged.

**Keywords:** agostic interactions · alkaline earth metals · hydroamination · ligands · metathesis

[1] *Catalytic Heterofunctionalization: from Hydroamination to Hydrozirconation* (Eds.: A. Togni, H. Grützmacher), Wiley-VCH, Weinheim, 2001.

[2] T. E. Müller, M. Beller, *Chem. Rev.* **1998**, *98*, 675.

[3] S. Hong, T. J. Marks, *Acc. Chem. Res.* **2004**, *37*, 673.

- [4] T. E. Müller, K. C. Hultzsich, M. Yus, F. Foubelo, M. Tada, *Chem. Rev.* **2008**, *108*, 3795.
- [5] K. D. Hesp, M. Stradiotto, *ChemCatChem* **2010**, *2*, 1192.
- [6] J. S. Ryu, G. Y. Li, T. J. Marks, *J. Am. Chem. Soc.* **2003**, *125*, 12584.
- [7] S. Harder, *Chem. Rev.* **2010**, *110*, 3852.
- [8] A. G. M. Barrett, M. R. Crimmin, M. S. Hill, P. A. Procopiu, *Proc. R. Soc. A* **2010**, *466*, 927.
- [9] R. Shannon, *Acta Crystallogr. Sect. A* **1976**, *32*, 751.
- [10] A. G. M. Barrett, C. Brinkmann, M. R. Crimmin, M. S. Hill, P. Hunt, P. A. Procopiu, *J. Am. Chem. Soc.* **2009**, *131*, 12906.
- [11] C. Brinkmann, A. G. M. Barrett, M. S. Hill, P. A. Procopiu, *J. Am. Chem. Soc.* **2012**, *134*, 2193.
- [12] B. Liu, T. Roisnel, J.-F. Carpentier, Y. Sarazin, *Angew. Chem.* **2012**, *124*, 5027; *Angew. Chem. Int. Ed.* **2012**, *51*, 4943.
- [13] B. Liu, T. Roisnel, J.-F. Carpentier, Y. Sarazin, *Chem. Eur. J.* **2013**, *19*, 13445.
- [14] M. R. Crimmin, M. Arrowsmith, A. G. M. Barrett, I. J. Casely, M. S. Hill, P. A. Procopiu, *J. Am. Chem. Soc.* **2009**, *131*, 9670.
- [15] M. Arrowsmith, M. R. Crimmin, A. G. M. Barrett, M. S. Hill, G. Kociok-Köhn, P. A. Procopiu, *Organometallics* **2011**, *30*, 1493.
- [16] S. Datta, P. W. Roesky, S. Blechert, *Organometallics* **2007**, *26*, 4392.
- [17] S. Datta, M. T. Gamer, P. W. Roesky, *Organometallics* **2008**, *27*, 1207.
- [18] J. Jenter, R. Köppe, P. W. Roesky, *Organometallics* **2011**, *30*, 1404.
- [19] J. S. Wixey, B. D. Ward, *Chem. Commun.* **2011**, *47*, 5449.
- [20] J. S. Wixey, B. D. Ward, *Dalton Trans.* **2011**, *40*, 7693.
- [21] T. D. Nixon, B. D. Ward, *Chem. Commun.* **2012**, *48*, 11790.
- [22] B. Liu, T. Roisnel, J.-F. Carpentier, Y. Sarazin, *Chem. Eur. J.* **2013**, *19*, 2784.
- [23] M. Arrowsmith, M. S. Hill, G. Kociok-Köhn, *Organometallics* **2009**, *28*, 1730.
- [24] M. Arrowsmith, A. Heath, M. S. Hill, P. B. Hitchcock, G. Kociok-Köhn, *Organometallics* **2009**, *28*, 4550.
- [25] Poly(indazolyl)borates are represented as benzopyrazolylborates, Tp<sup>Bo</sup>, and the fusion of the benzo ring to pz (3,4- or 4,5) is denoted by a superscript of 3 or 4 preceding "Bo"; see C. Pettinari, *Scorpionates II: Chelating Borate Ligands*, Imperial College Press, London, **2008**.
- [26] E. Despagnet-Ayoub, K. Jacob, L. Vendier, M. Etienne, E. Alvarez, A. Caballero, M. M. Díaz-Requejo, P. J. Pérez, *Organometallics* **2008**, *27*, 4779.
- [27] A. Caballero, E. Despagnet-Ayoub, M. M. Díaz-Requejo, A. Díaz-Rodríguez, M. E. González-Núñez, R. Mello, B. K. Muñoz, W.-S. Ojo, G. Asensio, M. Etienne, P. J. Pérez, *Science* **2011**, *332*, 835.
- [28] W.-S. Ojo, K. Jacob, E. Despagnet-Ayoub, B. K. Muñoz, S. Gonell, L. Vendier, V.-H. Nguyen, M. Etienne, *Inorg. Chem.* **2012**, *51*, 2893.
- [29] B. K. Muñoz, W.-S. Ojo, K. Jacob, N. Romero, L. Vendier, E. Despagnet-Ayoub, M. Etienne, *New J. Chem.* **2014**, *38*, 2451.
- [30] S.-C. Roşca, T. Roisnel, V. Dorcet, J.-F. Carpentier, Y. Sarazin, *Organometallics* **2014**, *33*, 5630.
- [31] N. Romero, L. Vendier, C. Dinoi, M. Etienne, *Dalton Trans.* **2014**, *43*, 10114.
- [32] M. H. Chisholm, *Inorg. Chim. Acta* **2009**, *362*, 4284.
- [33] M. H. Chisholm, J. C. Gallucci, K. Phomphrai, *Inorg. Chem.* **2004**, *43*, 6717.
- [34] M. H. Chisholm, J. Gallucci, K. Phomphrai, *Chem. Commun.* **2003**, 48.
- [35] X. Xu, Y. Chen, G. Zou, Z. Ma, G. Li, *J. Organomet. Chem.* **2010**, *695*, 1155.
- [36] A. Torvisco, A. Y. O'Brien, K. Ruhlandt-Senge, *Coord. Chem. Rev.* **2011**, *255*, 1268.
- [37] S. Trofimenko, *Scorpionates: The Coordination Chemistry of Polypyrazolylborate Ligands*, Imperial College Press, London, **1999**.
- [38] C. Müller, H. Görls, S. Kriek, M. Westerhausen, *Eur. J. Inorg. Chem.* **2013**, 5679.
- [39] S. Sarish, S. Nembenna, S. Nagendran, H. W. Roesky, A. Pal, R. Herbst-Irmer, A. Ringe, J. Magull, *Inorg. Chem.* **2008**, *47*, 5971.
- [40] B. Cordero, V. Gómez, A. E. Platero-Prats, M. Revés, J. Echeverría, E. Cremades, F. Barragán, S. Alvarez, *Dalton Trans.* **2008**, 2832.
- [41] O. Michel, H. M. Dietrich, R. Litlabø, K. W. Törnroos, C. Maichle-Mössmer, R. Anwender, *Organometallics* **2012**, *31*, 3119.
- [42] M. S. Hill, P. B. Hitchcock, *Chem. Commun.* **2003**, 1758.
- [43] J. S. Alexander, K. Ruhlandt-Senge, H. Hope, *Organometallics* **2003**, *22*, 4933.
- [44] A. G. M. Barrett, M. R. Crimmin, M. S. Hill, G. Kociok-Köhn, D. J. MacDougall, M. F. Mahon, P. A. Procopiu, *Organometallics* **2008**, *27*, 3939.
- [45] Y. Sohrin, M. Matsui, Y. Hata, H. Hasegawa, H. Kokusen, *Inorg. Chem.* **1994**, *33*, 4376.
- [46] M. J. Saly, M. J. Heeg, C. H. Winter, *Inorg. Chem.* **2009**, *48*, 5303.
- [47] W. A. Herrmann, J. Eppinger, M. Spiegler, O. Runte, R. Anwender, *Organometallics* **1997**, *16*, 1813.
- [48] R. Anwender, O. Runte, J. Eppinger, G. Gerstberger, E. Herdtweck, M. Spiegler, *J. Chem. Soc. Dalton Trans.* **1998**, 847.
- [49] W. Hieringer, J. Eppinger, R. Anwender, W. A. Herrmann, *J. Am. Chem. Soc.* **2000**, *122*, 11983.
- [50] C. Meermann, G. Gerstberger, M. Spiegler, K. W. Törnroos, R. Anwender, *Eur. J. Inorg. Chem.* **2008**, 2014.
- [51] H. F. Yuen, T. J. Marks, *Organometallics* **2008**, *27*, 155.
- [52] Y. Sarazin, D. Roşca, V. Poirier, T. Roisnel, A. Silvestru, L. Maron, J.-F. Carpentier, *Organometallics* **2010**, *29*, 6569.
- [53] M. Westerhausen, *Inorg. Chem.* **1991**, *30*, 96.
- [54] E. D. Brady, T. P. Hanusa, M. Pink, V. G. Young, *Inorg. Chem.* **2000**, *39*, 6028.
- [55] A. M. Johns, S. C. Chmely, T. P. Hanusa, *Inorg. Chem.* **2009**, *48*, 1380.
- [56] H. Shanan-Atidi, K. H. Bar-Eli, *J. Phys. Chem.* **1970**, *74*, 961.
- [57] H. S. Gutowsky, C. H. Holm, *J. Chem. Phys.* **1956**, *25*, 1228.
- [58] J. Eppinger, M. Spiegler, W. Hieringer, W. A. Herrmann, R. Anwender, *J. Am. Chem. Soc.* **2000**, *122*, 3080.
- [59] L. Procopio, P. Carroll, D. Berry, *J. Am. Chem. Soc.* **1994**, *116*, 177.
- [60] K. Yan, G. Schoendorff, B. M. Upton, A. Ellern, T. L. Windus, A. D. Sadow, *Organometallics* **2013**, *32*, 1300.
- [61] J. Hitzbleck, G. B. Deacon, K. Ruhlandt-Senge, *Angew. Chem. Int. Ed.* **2004**, *43*, 5218; *Angew. Chem.* **2004**, *116*, 5330.
- [62] E. Hollink, P. R. Wei, D. W. Stephan, *Can. J. Chem.* **2005**, *83*, 430.
- [63] C. A. Zechmann, T. J. Boyle, M. A. Rodriguez, R. A. Kemp, *Polyhedron* **2000**, *19*, 2557.
- [64] C. A. Zechmann, T. J. Boyle, M. A. Rodriguez, R. A. Kemp, *Inorg. Chim. Acta* **2001**, *319*, 137.
- [65] M. Westerhausen, M. H. Digeser, B. Wieneke, H. Nöth, J. Knizek, *Eur. J. Inorg. Chem.* **1998**, 517.
- [66] I. Nagl, W. Scherer, M. Tafipolsky, R. Anwender, *Eur. J. Inorg. Chem.* **1999**, 1405.
- [67] G. W. Rabe, A. L. Rheingold, C. D. Incarvito, *Z. Kristallogr. New Cryst. Struct.* **2000**, *215*, 560.
- [68] A. M. Bienfait, C. Schädle, C. Maichle-Mössmer, K. W. Törnroos, R. Anwender, *Dalton Trans.* **2014**, *43*, 17324.
- [69] B. Liu, T. Roisnel, J.-P. Guegan, J.-F. Carpentier, Y. Sarazin, *Chem. Eur. J.* **2012**, *18*, 6289.
- [70] K. Yan, B. M. Upton, A. Ellern, A. D. Sadow, *J. Am. Chem. Soc.* **2009**, *131*, 15110.
- [71] J. F. Dunne, D. B. Fulton, A. Ellern, A. D. Sadow, *J. Am. Chem. Soc.* **2010**, *132*, 17680.
- [72] X. Zhang, T. J. Emge, K. C. Hultzsich, *Angew. Chem. Int. Ed.* **2012**, *51*, 394; *Angew. Chem.* **2012**, *124*, 406.
- [73] S. Tobisch, *Chem. Eur. J.* **2011**, *17*, 14974.
- [74] S. Tobisch, *Dalton Trans.* **2012**, *41*, 9182.
- [75] S. Tobisch, *Chem. Eur. J.* **2014**, *20*, 8988.
- [76] Attempts to perform cyclohydroamination catalysis with complex **5** were unsuccessful: Strictly no activity was observed. This is most likely due to catalyst decomposition under catalytic conditions, by dehydrocoupling of Si-H (in the {N(SiMe<sub>2</sub>H)} ligand framework) and H-N (in the substrate) bonds, leading to the formation of a new N-Si bond and release of dihydrogen. This is a largely detrimental phenomenon that we have already observed and abundantly discussed with other related alkaline-earth complexes; see reference [22].
- [77] Y. Tamaru, M. Hojo, H. Higashimura, Z. Yoshida, *J. Am. Chem. Soc.* **1988**, *110*, 3994.
- [78] J. Boncella, C. Coston, J. Cammack, *Polyhedron* **1991**, *10*, 769.
- [79] P. Tanner, D. Burkey, T. Hanusa, *Polyhedron* **1995**, *14*, 331.
- [80] A. Altomare, G. Cascarano, C. Giacovazzo, A. Guagliardi, *J. Appl. Crystallogr.* **1993**, *26*, 343.
- [81] G. M. Sheldrick, *Acta Crystallogr. Sect. A* **2008**, *64*, 112.
- [82] L. J. Farrugia, *J. Appl. Crystallogr.* **1999**, *32*, 837.

Received: September 29, 2014

Published online on January 23, 2015